

DOKUZ EYLÜL UNIVERSITY
GRADUATE SCHOOL OF NATURAL AND APPLIED
SCIENCES

INVESTIGATION OF THERMOPHYSICAL
PROPERTIES OF NANOFUIDS

by
Alpaslan TURGUT

January, 2010
İZMİR

INVESTIGATION OF THERMOPHYSICAL PROPERTIES OF NANOFLUIDS

**A Thesis Submitted to the
Graduate School of Natural and Applied Sciences of Dokuz Eylül University
In Partial Fulfillment of the Requirements for the Degree of Doctor of
Philosophy in Mechanical Engineering, Energy Program**

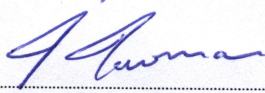
**by
Alpaslan TURGUT**

January, 2010

İZMİR

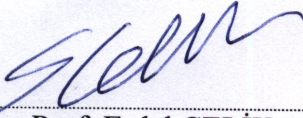
Ph.D. THESIS EXAMINATION RESULT FORM

We have read the thesis entitled “**INVESTIGATION OF THERMOPHYSICAL PROPERTIES OF NANOFLUIDS**” completed by **ALPASLAN TURGUT** under supervision of **PROF. DR. İSMAİL HAKKI TAVMAN** and we certify that in our opinion it is fully adequate, in scope and in quality, as a thesis for the degree of Doctor of Philosophy.



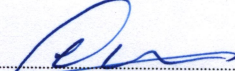
Prof. Dr. İsmail Hakkı TAVMAN

Supervisor



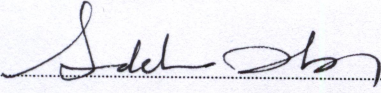
Assoc. Prof. Erdal ÇELİK

Thesis Committee Member



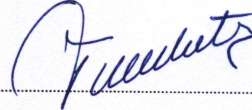
Assoc. Prof. Aytunç EREK

Thesis Committee Member



Prof. Dr. Sadık Kakaş

Examining Committee Member



Assoc. Prof. Dr. Dilek KUMLU TAŞ

Examining Committee Member

Prof. Dr. Cahit HELVACI

Director

Graduate School of Natural and Applied Sciences

ACKNOWLEDGMENTS

I give sincere appreciation and thanks to my supervisor Prof. Dr. İsmail Tavman for his continuous encouragement, valuable advice and support throughout the course of this study. I would also like to thank Assoc. Prof. Erdal Çelik and Assoc. Prof. Aytunç Erek for the useful discussions on periodical meetings of this research.

I want to express my gratitude to Prof. Dr. Mihai Chirtoc for the opportunity he provided for me to stay in Thermophysical Characterization Laboratory, Grespi, University of Reims, France. He has taught me a lot on experimental work. Also I thank Dr. Jean-Stephene Antoniow and Dr. Jean-François Henry for helpful consultation during my stay in Reims.

I have received tremendous assistance from Dr. Levent Çetin during configuration of the experimental setup for thermal conductivity measurements.

I also would like to thank Prof. Dr. Kliment Hadjov for involving me into an international project which has given to me the chance for deep discussions on the subject with other partners. I must also thank to Prof. Dr. Şebnem Tavman for useful discussion on production of nanofluids. I particularly acknowledge the support and encouragement of Assoc. Prof. Dilek Kumlutaş, Dr. Tahsin Başaran, Ziya Haktan Karadeniz, Mehmet Akif Ezan and Alim Zorluol.

I acknowledge the financial support of TUBITAK (project no:107M160), Research Foundation of Dokuz Eylul University (project no:2009.KB.FEN.018) and Agence Universitaire de la Francophonie (project no:AUF-PCSI 6316 PS821).

Most of all, I thank my parents and parents-in-law for all of the encouragement and support they have provided. Lastly, I would like to dedicate this thesis to my wonderful wife Ferika, who continuously have been supporting my study and life.

Alpaslan TURGUT

INVESTIGATION OF THERMOPHYSICAL PROPERTIES OF NANOFLUIDS

ABSTRACT

Nanofluids are liquid suspensions of particles with at least one of their dimensions smaller than 100 nanometer (nm). Nanofluid technology becomes a new challenge for the heat transfer fluid since it has been reported that the thermal conductivity of nanofluid is anomalously enhanced at a very low volume fraction of nanoparticles.

In this study, a new application of a hot wire sensor for measurement of thermal conductivity of (nano)fluids, based on a hot wire thermal probe with ac excitation and 3 omega lock-in detection, were presented. Due to modulated heat flow in cylindrical geometry with a radius comparable to the thermal diffusion length, the necessary sample quantity is kept very low, typically 25 microliter. The thermal conductivities of de-ionized water based TiO₂, SiO₂, Al₂O₃ nanofluids and ethylene glycol based Al₂O₃ nanofluids were measured and their dependence of particle volume fraction and temperature were investigated. Our results show that thermal conductivity values are inside the limits of (moderately lower than) Hamilton-Crosser model. Our experiments at different temperatures show that relative thermal conductivity of nanofluids is not related with the temperature of the fluid.

For industrial applications of nanofluids, one should also know the viscosity characteristics, since for heat transfer applications pump costs are important. We investigated the temperature dependent viscosity of nanofluids for different particle concentrations by a Sine-wave Vibro Viscometer. Viscosity of our nanofluids increase dramatically with the increase in particle concentration, Einstein model is found to be unable to predict this increase.

Keywords: 3 omega method, Nanofluid, Thermal conductivity, Viscosity

NANOAKIŞKANLARIN TERMOFİZİKSEL ÖZELLİKLERİNİN ARAŞTIRILMASI

ÖZ

Herhangi bir boyutu 100 nanometreden (nm) daha küçük olan tanecikleri içeren süspansiyonlar nanoakışkan olarak adlandırılmaktadır. Çok az miktarlardaki nanotanecik hacimsel katkı oranlarında bile baz akışkana göre oldukça yüksek ısı iletkenlik kabiliyetine sahip olduğu belirtilen nanoakışkanlar yeni nesil ısı transfer akışkanı olma potansiyeli ile önem kazanmaktadır.

Çalışma kapsamında ilk olarak (nano)akışkanların ısı iletim katsayılarının ölçümünde kullanılmak üzere, alternatif akım uyarımlı ve 3. harmoniğin (3 omega) kilitlemeli yükseltici ile belirlenmesi prensibine dayalı ölçme sisteminin yeni bir uygulaması sunulmuştur. Yarıçapın ısı yayılım uzunluğundan yeterince küçük olduğu silindirik bir geometride modüle edilmiş ısı akısı sayesinde, ölçüm için 25 mikrolitre miktarında numune yeterli olmaktadır. Bu yöntemle su bazlı TiO₂, SiO₂, Al₂O₃ ve etilen glikol bazlı Al₂O₃ nanoakışkanların ısı iletkenlikleri farklı hacimsel katkı oranlarında ve farklı sıcaklıklarda incelenmişlerdir. Elde edilen sonuçlar, Hamilton – Crosser modeliyle uyumludur, ancak biraz daha düşük seviyelerde ısı iletkenlik artışı olduğu görülmüştür. Farklı sıcaklıklarda yapılan ölçümlerden ise, nanoakışkanın bağlı ısı iletkenliğinin akışkanın sıcaklığı ile bir değişim göstermediği sonucu elde edilmiştir.

Isı transferi uygulamalarında soğutucu sıvının pompa işletme maliyetleri önemli olduğu için nanoakışkanların viskozite değerlerinin de bilinmesi önemlidir. Farklı tanecik hacimsel katkı oranlarındaki nanoakışkanların viskoziteleri değişik sıcaklıklarda Sine-wave Vibro Viscometer ile ölçülmüştür. Tanecik katkı oranı arttıkça nanoakışkanların viskozitelerinin önemli ölçüde arttığı ve bu artışın Einstein modeli ile tahmin edilemediği görülmüştür.

Anahtar sözcükler : 3 omega yöntemi, Nanoakışkan, Isıl iletkenlik, Viskozite

CONTENTS

	Page
Ph.D. THESIS EXAMINATION RESULT FORM	ii
ACKNOWLEDGEMENTS	iii
ABSTRACT	iv
ÖZ	v
CHAPTER ONE – INTRODUCTION	1
1.1 Nanofluids	1
1.2 Motivation	3
1.3 Objectives	6
1.4 Outline of Research	6
CHAPTER TWO – LITERATURE REVIEW	7
2.1 Methods for Measuring Thermal Conductivity of Nanofluids.....	7
2.2 Synthesis of Nanofluids.....	10
2.3 Thermal Conductivity Enhancement in Nanofluids	11
2.4 Possible Mechanisms and Models for Effective Thermal Conductivity of Nanofluids	13
2.4.1 Brownian Motion of Particles.....	14
2.4.2 Molecular-level Layering of the Liquid at the Liquid/Particle Interface	15
2.4.3 Nature of Heat Transport in Nanoparticles.....	17
2.4.4 Effects of Nanoparticle Clustering	17
2.5 Viscosity of Nanofluids.....	18

CHAPTER THREE – 3 ω METHOD FOR MEASURING THERMAL CONDUCTIVITY OF (NANO)FLUIDS	21
3.1 Introduction	21
3.2 Theoretical Background	22
3.2.1 3- ω Signal Generation	22
3.2.2 Interface Thermal Impedance	24
3.2.3 Data Reduction Method	25
3.3 Experimental	25
3.4 Results and Discussion	27
3.5 Conclusion	29
CHAPTER FOUR – PROCESSING OF NANOFLUIDS.....	30
4.1 Introduction	30
4.2 Properties of Particles and Basefluids	31
4.3 Preparation of Nanofluids	32
4.4 Zeta Potential of Nanofluids.....	33
CHAPTER FIVE – THERMAL CONDUCTIVITY OF NANOFLUIDS	35
5.1 Introduction	35
5.2 Materials	36
5.3 Results and Discussion	36
5.3.1 Effect of Ultrasonication Time	36
5.3.2 Effect of Volume Fraction and Temperature	37
5.3.2.1 SiO ₂ – water Nanofluids	37
5.3.2.2 TiO ₂ – water Nanofluids	39
5.3.2.3 Al ₂ O ₃ – water Nanofluids	44
5.3.2.3 Al ₂ O ₃ – ethylene glycol Nanofluids.....	48

5.3.3 Effect of Particle Conductivity	51
5.3.4 Effect of Surfactant.....	51
5.3.5 Effect of Basefluid.....	52
5.4 Conclusion.....	53
CHAPTER SIX – VISCOSITY OF NANOFUIDS	55
6.1 Introduction	55
6.2 Materials	56
6.3 Experimental Setup and Procedure	57
6.4 Results and Discussion.....	59
6.4.1 Effect of Volume Fraction and Temperature.....	59
6.4.1.1 SiO ₂ – water Nanofluids	59
6.4.1.2 TiO ₂ – water Nanofluids	61
6.4.1.3 Al ₂ O ₃ – water Nanofluids	64
6.4.1.4 Al ₂ O ₃ – ethylene glycol Nanofluids.....	67
6.4.2 Effect of Basefluid.....	70
6.5 Conclusion.....	71
CHAPTER SEVEN – CONCLUSIONS	73
7.1 3- ω Method	73
7.2 Nanofluids	74
REFERENCES.....	77

CHAPTER ONE

INTRODUCTION

1.1 Nanofluids

Nanofluids are solid nanoparticles or nanofibers in suspension in a base fluid. To be qualified as nanofluid it is generally agreed that at least one size of the solid particle be less than 100nm. Various industries such as transportation, electronics, food, medical industries require efficient heat transfer fluids to either evacuate or transfer heat by means of a flowing fluid. Especially with the miniaturization in electronic equipments, the need for heat evacuation has become more important in order to ensure proper working conditions for these elements. Thus, new strategies, such as the use of new, more conductive fluids are needed. Most of the fluids used for this purpose are generally poor heat conductors compared to solids, (Figure 1.1).

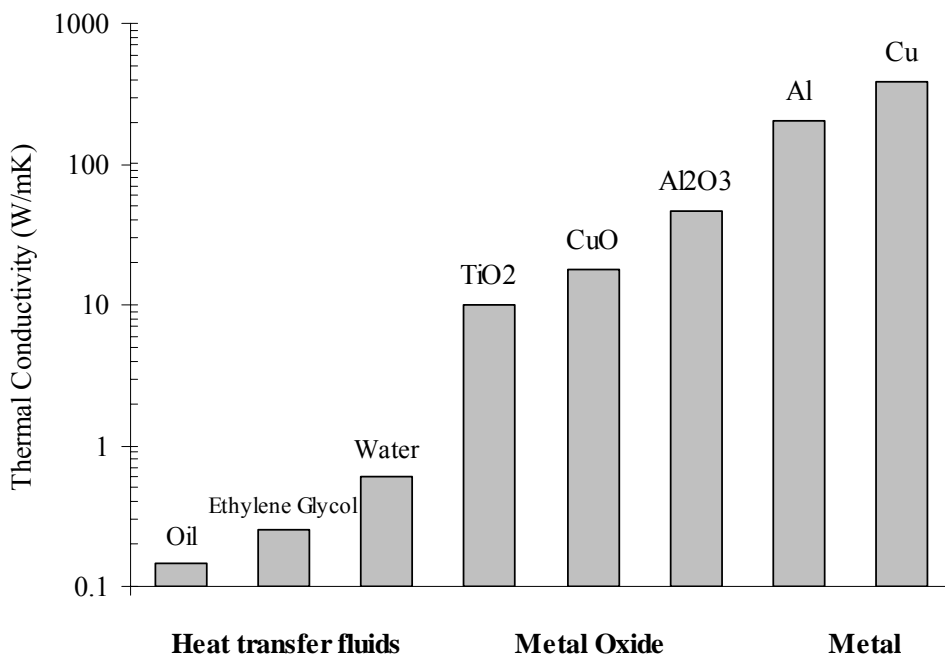


Figure 1.1 Thermal conductivity of typical materials (solids and liquids) at 300 K

It is well known that fluids may become more conductive by the addition of conductive solid particles. However such mixtures have a lot of practical limitations,

primarily arising from the sedimentation of particles and the associated blockage issues. These limitations can be overcome by using suspensions of nanometer-sized particles (nanoparticles) in liquids, known as nanofluids. After the pioneering work by Choi of the Argonne National Laboratory, U.S.A. in 1995 (Choi, 1995) and his publication (Choi, Zhang, Yu, Lockwood & Grulke, 2001) reporting an anomalous increase in thermal conductivity of the base fluid with the addition of low volume fractions of conducting nanoparticles, there has been a great interest for nanofluids research both experimentally and theoretically. More than 1000 nanofluid-related research publications have appeared in literature since then and the number per year appears to be increasing as it can be seen from Figure 1.2. In 2008 alone, 282 research papers were published in *Science Citation Index* journals. However, the transition to industrial practice requires that nanofluid technology become further developed, and that some key barriers, like the stability and sedimentation problems be overcome.

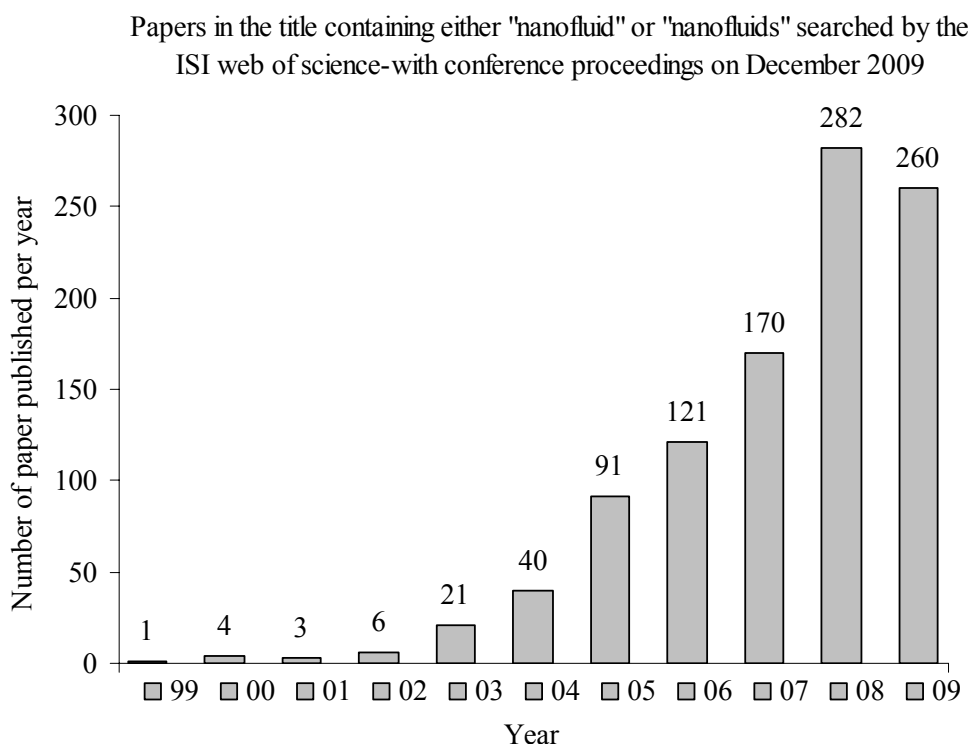


Figure 1.2 Publications on nanofluids since 1999.

1.2 Motivation

The first publications on thermal conductivity of nanofluids were with base fluids water or ethylene-glycol (EG) and with nanoparticles such as aluminum-oxide (Al_2O_3) (Lee, Choi, Li & Eastman 1999; Wang, Xu & Choi, 1999; Xie, Wang, Xi, Liu & Ai, 2002; Das, Putra, Thiesen & Roetzel, 2003), copper-oxide (CuO) (Lee et al., 1999; Wang et al., 1999; Das et al., 2003), titanium-dioxide (TiO_2) (Murshed, Leong & Yang, 2005), copper (Cu) (Xuan & Li, 2000; Eastman, Choi, Li, Yu & Thompson, 2001). They all measured great enhancement in thermal conductivity for low particles addition, typical enhancement was in the 5–60% range over the base fluid for 0.1–5% nanoparticles volume concentrations in various liquids. These unusual results have attracted great interest both experimentally and theoretically from many research groups because of their potential benefits and applications for cooling in many industrials from electronics to transportation. Recent papers provide detailed reviews on all aspects of nanofluids, including preparation, measurement and modeling of thermal conductivity and viscosity (Murshed, Leong & Yang, 2008a; Yu, France, Routbort & Choi, 2008; Wang & Mujumdar, 2008; Choi, 2009). Very few studies (Masuda, Ebata, Teramae & Hishinuma, 1993; Das et al., 2003; Chon & Khim, 2005; Li & Peterson, 2006; Wang, Tang, Liu, Zheng & Araki, 2007; Zhang, Gu & Fujii, 2006) have been performed to investigate the temperature effect on the effective thermal conductivity of nanofluids. On relative thermal conductivity of TiO_2 -water nanofluids, no temperature effect has been found in the study by Masuda et al. (1993) and Zhang et al. (2006). However, Wang et al. (2007) measured an increase in relative thermal conductivity for the same nanofluid. Hence, to confirm the effects of temperature on the relative thermal conductivity of nanofluids, more experimental studies are essential. The experimental data reported in the literature is very scattered, for the same base fluid and the same particles there are many different results. Some researchers (Masuda et al., 1993; Zhang et al., 2006; Wang et al., 2007) measured only a moderate increase of effective thermal conductivity with the addition of nanoparticles. Their experimental results can be explained by classical Maxwell (1881) or Hamilton & Crosser (1962) models for mixtures. A recent publication by Koblinski, Prasher & Eapen (2008) reveals this

controversy about the scatter of experimental data and compares the experimental data from different authors for various water based nanofluids. He shows that this results fall within the upper and lower limits of classical two phase mixture theories.

The different techniques for measuring the thermal conductivity of liquids can be classified into two main categories: steady-state and transient methods. Both of these methods have some merits and disadvantages. The equipment for steady state method is simple and the governing equations for heat transfer are well known and simple. The main disadvantage is the very long experimental times required for the measurement and the necessity to keep all the conditions stable during this time. For nanofluids, the steady state methods are not very adequate, during the long measurement time particles may settle down; it is extremely difficult to keep everything stable during the experimental run. That is the reason why there are very few studies on thermal conductivity of nanofluids with steady state methods. Wang et al. (1999) measured the effective thermal conductivity of metal oxide nanoparticle suspensions using a steady-state method. Somewhat later, Das and co-workers (Das et al., 2003) measured the effective thermal conductivity of metal and metal oxide nanoparticle suspensions using a temperature oscillation method.

The transient hot wire (THW) method has been widely used for measurements of the thermal conductivities and, in some cases, the thermal diffusivities of fluids with a high degree of accuracy (Nagasaka & Nagashima, 1981; Xie et al., 2002). More than 80% of the thermal conductivity measurements on nanofluids were performed by transient hot wire method (Masuda et al., 1993; Xie et al., 2002; Murshed et al., 2005; Zhang et al., 2006; Yoo, Hong & Yang, 2007; He et al., 2007; Assael, Chen, Metaxa & Wakeham, 2004). However, (Vadasz, Govender & Vadasz, 2005) expressed that the significant enhancement of effective thermal conductivity of nanofluids obtained using the hot-wire method could be the result of the thermal wave effect of hyperbolic heat conduction used in the temperature change calculation. Li, Williams, Buongiorno, Hu & Peterson (2008), showed that at the higher temperature, the values of the relative effective thermal conductivities at the same volume fraction tested by the transient hot-wire method were much higher than

the corresponding values tested by steady-state cut-bar method. They explained that the onset of natural convection was one of the possibilities for this effect and it was much more evident at the higher temperatures. Also the groups (Putnam, Cahill, Braun, & Shimmin, 2006; Rusconi, Rodari & Piazza, 2007) that utilized optical measurement methods did not observe significant enhancement of thermal conductivity of nanofluids which were well agree with Maxwell model.

Although some review articles (Eastman, Phillpot, Choi & Keblinski, 2004; Keblinski, Eastman & Cahill, 2005; Das, Choi & Patel, 2006) emphasized the importance of investigating the viscosity of nanofluids, very few studies on effective viscosity were reported. Viscosity is as critical as thermal conductivity in engineering systems that employ fluid flow. Pumping power is proportional to the pressure drop, which in turn is related to fluid viscosity. More viscous fluids require more pumping power. In laminar flow, the pressure drop is directly proportional to the viscosity. Masuda et al. (1993), measured the viscosity of TiO₂-water nanofluids suspensions, they found that for 27 nm TiO₂ particles at a volumetric concentration of 4.3% the viscosity increased by 60% with respect to pure water. In his work on the effective viscosity of Al₂O₃-water nanofluids, Wang et al. (1999) measured an increase of about 86% for 5 vol% of 28 nm nanoparticles content. In their case, a mechanical blending technique was used for dispersion of Al₂O₃ nanoparticles in distilled water. They also measured an increase of about 40% in viscosity of ethylene glycol at a volumetric loading of 3.5% of Al₂O₃ nanoparticles. (Das, Putra & Roetzel, 2003) and (Putra, Roetzel & Das, 2003) measured the viscosity of water-based nanofluids, for Al₂O₃ and CuO particles inclusions, as a function of shear rate they both showed Newtonian behavior for a range of volume percentage between 1% and 4%. They also observed an increase in viscosity with an increase of particle volume fraction, for Al₂O₃/water-based nanofluids. In all cases the viscosity results were significantly larger than the predictions from the classical theory of suspension rheology such as Einstein's model (Einstein, 1956).

1.3 Objectives

The objective of the present research is to study the influence of some parameters such as particle volume fraction, temperature, thermal conductivities of base fluids and particles on the effective thermal conductivity and effective viscosity of nanofluids. The secondary objective is to build a hot wire sensor and develop a data reduction method based on ac excitation and lock-in detection for measurement of thermal conductivity of (nano)fluids.

1.4 Outline of Research

The thesis is divided into seven chapters. In chapter one a short introduction to nanofluids is given. Also the objectives of this research are proposed. In chapter two, a brief literature review on nanofluids is presented. Theoretical background and validation of 3ω method for measuring thermal conductivity of (nano)fluids are presented in chapter three. Properties of the materials used in production of nanofluids and details about the production process will be given in chapter four. Our experimental results for measuring effective thermal conductivity and effective viscosity of nanofluids are given in chapter five and chapter six, respectively. Also the principle of the vibro viscometer for measurement of viscosity presented in chapter six. In chapter seven, the concluding remarks are summarized and future works are recommended for 3ω method and nanofluids.

CHAPTER TWO

LITERATURE REVIEW

In the last five years, some review articles (Eastman et al. (2004); Das et al. (2006); Trisaksri & Wongwises (2007); Wang & Mujumdar (2007); Yu et al. (2008); Murshed et al. (2008b); Wen, Lin, Vafaei & Zhang (2009); Kakac & Pramuanjaroenkij (2009); Chandrasekar, M., & Suresh (2009); Li et al. (2009); Ozerinc, Kakac & Yazicioglu (2009)) were published. Although these review papers have generally covered the current aspects of experimental and theoretical studies of nanofluids, the state-of-the-arts on nanofluids need to be re-surveyed due to a great number of new papers on nanofluids published, in those some new phenomena and new findings are reported(Li et al., 2009). In this chapter we have reviewed some important titles such as methods for measuring thermal conductivity of nanofluids, synthesis of nanofluids, thermal conductivity of nanofluids, mechanisms and models for effective thermal conductivity of nanofluids and viscosity of nanofluids.

2.1 Methods for Measuring Thermal Conductivity of Nanofluids

As it is mentioned in chapter one, most of the experimental study on thermal conductivity of nanofluids are measured by transient hot wire method(Masuda et al. (1993); Lee et al. (1999); Eastman et al. (2001); Choi et al. (2001); Xie et al. (2002); Patel et al. (2003); Wen & Ding (2004); Murshed et al. (2005); Hong et al. (2006); Hwang et al. (2006), Kang et al. (2006); Zhang et al. (2006); Yoo et al. (2007); He et al. (2007); Murshed et al. (2008b); Lee et al. (2008)). The measurement principle of the transient hot wire technique is based on the calculation of the transient temperature field around a thin wire, which can be treated as a line source. A constant current is supplied to the wire to generate the necessary temperature rise. The wire is encircled by a sample nanofluid, whose thermal conductivity and thermal diffusivity are to be measured. The wire acts as both the heat source and the temperature sensor. The heat dissipated in the wire increases the temperature of the wire and also that of the sample. The temperature rise in the wire depends on the

thermal conductivity of the sample through which the wire is immersed (Murshed et al., 2005).

Parallel plate technique is a steady state method used by Wang et al. (1999) and Sinha et al. (2009) for measuring the thermal conductivity of nanofluids. In this method the fluid sample is located in a narrow gap between two parallel plates: an upper plate and a lower plate. The upper plate is surrounded by a guard ring and guard plate. A temperature difference across the fluid layer is established by generating heat in the upper plate. To minimize parasitic heat flows as much as possible, the guard ring and guard plate are kept at the same temperature as the upper plate by application of an appropriate amount of heat. The thermal conductivity of the fluid between the plates is deduced from the linearized version of the Fourier law of heat conduction (Sakonidou, van den Berg, ten Seldam & Sengers, 1999). Also steady state techniques such as cut-bar apparatus (Li & Peterson, 2006) or co-axial cylinder cell (Glory et al., 2008) are employed for the measurement of thermal conductivity of nanofluids.

The temperature oscillation technique (Bhattacharya et al., 2006) to measure the thermal diffusivity of a fluid consists of filling a cylindrical volume with the fluid, applying an oscillating temperature boundary condition at the two ends of the cylinder, measuring the amplitude and phase of the temperature oscillation at any point inside the cylinder, and finally calculating the fluid thermal diffusivity from the amplitude and phase values of the temperature oscillations at the ends and at the point inside the cylinder, used for measurement of nanofluids by Das, Putra, Thiesen et al. (2003).

Another method for measuring thermal diffusivity is the flash method developed by Parker, Jenkins, Butler & Abbott (1961) and successfully used for the thermal diffusivity measurement of solid materials. A high intensity short duration heat pulse is absorbed in the front surface of a thermally insulated sample of a few millimeters thick. The sample is coated with absorbing black paint if the sample is transparent to the heat pulse. The resulting temperature of the rear surface is measured by a

thermocouple or infrared detector, as a function of time and is recorded either by an oscilloscope or a computer having a data acquisition system. The thermal diffusivity is calculated from this time-temperature curve and the thickness of the sample. This method is commercialized now, and there are ready made apparatus with sample holders for fluids. There is only one publication on nanofluids with this method, Shaikh, Lafdi & Ponnappan (2007) measured thermal conductivity of carbon nanoparticle doped PAO oil.

Besides these methods mentioned above, there are few optical techniques for measurements of thermal properties of nanofluids. Venerus, Kabadi, Lee & Perez-Luna (2006), used forced Rayleigh scattering method. Putnam et al. (2006) employed an optical beam deflection technique. Another optical technique is used by Rusconi et al. (2006), called thermal lensing (TL). TL is a self-effect on beam propagation taking place when a focused laser beam heats up a partially absorbing sample. Thermal expansion of the absorbing medium induces a local density distribution that, close to the beam center, has a simple parabolic shape. Such a radial density gradient produces, in turn, a quadratic refractive index profile, acting as a negative lens that increases the divergence of the transmitted beam, which can be measured by detecting changes of the central beam intensity (Rusconi et al. (2006)). Recently, Schmidt et al. (2008) used the transient grating technique relies on the thermal decay of a periodic variation in index of refraction generated by the interference of two picosecond light pulses. Although more time consuming than the hotwire method, it is noninvasive and can be used on much smaller samples. In addition, because the measurement occurs on a microsecond time scale, natural convection effects are avoided Schmidt et al. (2008).

There are also two studies (Li et al. (2008) and Schmidt et al. (2008)) that observe the effect of different measurement techniques on thermal conductivity of nanofluids. Li et al. (2008), show that at higher temperature, the values of the relative effective thermal conductivities at the same volume fraction tested by the transient hot-wire method were much higher than the corresponding values tested by steady-state cut-bar method. They explain that the onset of natural convection was one of the

possibilities for this effect and it was much more evident at the higher temperatures. Schmidt et al. (2008), investigated the effect of measurement technique on thermal conductivity of nanofluids by using the hotwire and transient grating techniques which are sufficiently different that it is unlikely they share common sources of systematic error. As a result they conclude that good agreement between the two measurements indicates that the observed enhancement in thermal conductivity can be trusted, and that either method can be a reliable way to measure the thermal conductivity of nanofluids (Schmidt et al., 2008).

2.2 Synthesis of Nanofluids

Modern technology allows the fabrication of materials at the nanometer scale, they are usually available in the market under different particle sizes and purity conditions. They exhibit unique physical and chemical properties compared to those of larger (micron scale and larger) particles of the same material. Nanoparticles can be produced from several processes such as gas condensation, mechanical attrition or chemical precipitation techniques (Trisaksri & Wongwises, 2007).

Nanofluids are generally produced by two different techniques: a one-step technique and a two-step technique. The one-step technique makes and disperses the nanoparticles directly into a base fluid simultaneously. Eastman et al. (2001), has used the direct evaporation condensation method which is the modification of inert gas condensation technique. Although this method has limitations of low vapor-pressure fluids and oxidations of pure metals, it provides perfect control over particle size and produces particles for stable nanofluids.

The two-step technique starts with nanoparticles which can usually be purchased and proceeds to disperse them into a base fluid. Most of the nanofluids containing oxide nanoparticles and carbon nanotubes reported in the literature are produced by the two-step process. The major advantage of the two-step technique is the possibility to use commercially available nanoparticles; this method provides an

economical way to produce nanofluids. Also it is suggested to use stabilizing agents during dispersion for stable nanofluids(Xuan & Li (2000)).

2.3 Thermal Conductivity Enhancement in Nanofluids

Since they are not expensive, alumina and copper oxides are the most common nanoparticles used by many researchers in nanofluid research. Lee et al. (1999), presented the thermal conductivity measurements on water and ethylene glycol (EG) that contained Al_2O_3 and CuO nanoparticles. They used volume fraction 1-5%, the enhancement they observed was 20% for CuO particles having 4% volume fraction in EG. When water is the base fluid the enhancement was 12%, at 3.5% CuO. Wang et al. (1999), measured the thermal conductivity of Al_2O_3 -water and CuO-water nanofluids having smaller particle size. They also used EG and engine oil (Pennzoil 10W-30) as the base fluids. The measurements showed the effect of particle size and method of dispersion. Xie et al. (2002), also with Al_2O_3 nanofluids observed the particle size effect.

Eastman et al. (1997), were the first to try (100 nm) copper particle-based nanofluids of transformer oil. They reported 55% enhancement with 5% volume fraction. The Argonne National Laboratory (ANL) group reported 40% enhancement with only 0.3% concentration of 10 nm copper particles suspended in EG (Eastman et al., 2001). This report clearly showed the particle size effect and potential of nanofluids with smaller particles. Hong, Hong & Yang (2006), obtained 18% enhancement with 0.55% volume fraction on Fe nanoparticles (10 nm), suspended in EG.

ANL group reported that, with 1% volume fraction of multi-walled carbon nanotubes, the enhancement of the thermal conductivity of engine oil is 150% (Choi et al., 2001). With polymer nanotubes, Biercuk et al. (2002), showed the similar enhancement.

Liu, Lin, Tsai & Wang (2006) reported that for 0.1% volume Cu-water nanofluid with spherical particles the enhancement varied between 11% and 23.8% depending on the grain size ranging from 75 to 300 nm, where a smaller grain size demonstrates increased enhancement ratio. Beck, Yuan, Warriar & Teja (2009) have measured the thermal conductivity of nanofluids containing seven sizes of alumina nanoparticles ranging from 8 to 282 nm in diameter. Contrary to the result of Liu et al. (2006), results of Beck et al. (2009) indicate that the thermal conductivity enhancement decreases as the particle size decreases below about 50 nm.

One important contribution on nanofluids was the discovery of a very strong temperature dependence of nanofluids (Das et al., 2003) with Al₂O₃ (38.4 nm) and CuO (28.6 nm) nanoparticles. They observed that a two to four fold increase in thermal conductivity take place over the temperature range of 21°C to 51°C. The results suggest the application of nanofluids as cooling fluids at higher temperature. Also results of Li & Peterson (2006) with Al₂O₃ (36 nm) water suspensions, demonstrated that temperature have significant effects on the thermal conductivity of the nanofluids. For Al₂O₃/water suspensions, increase in the mean temperature from 27 °C to 34.7°C results in an enhancement of nearly three times.

Patel et al. (2003) studied gold (Au) and silver (Ag) nanoparticles with thoriare and citrate as coatings in water- and toluene-based fluids. They found 5%-21% enhancement of the thermal conductivity of nanofluids for water with citrate in the temperature range 30–60°C at a very low loading of 0.00026 % vol. of Ag particles. For a loading of 0.011% of Au particles, the improvement of thermal conductivity was around 7%-14%.

Murshed et al. (2005), with TiO₂ nanoparticles observed a nonlinear dependence of enhancement in thermal conductivity on particle concentration at lower volume fractions. TiO₂ nanoparticles of rod-shape (ø10 × 40) and spherical shape (ø15) dispersed in deionized water. They observed nearly 33% and 30% enhancements of the effective thermal conductivity for TiO₂ particles of ø10 × 40 and ø15,

respectively. Both particle size and shape influenced the thermal conductivity of nanofluids.

All these results were high when compared with the Maxwell (1881) model or Hamilton and Crosser (1962) model.

2.4 Possible Mechanisms and Models for Effective Thermal Conductivity of Nanofluids

Dating back to the classical Maxwell model (Maxwell, 1881), many theoretical and empirical models have been proposed to predict the effective thermal conductivity of two phase mixtures. Using potential theory, Maxwell obtained a simple relationship for the conductivity of randomly distributed and non-interacting homogeneous spheres in a homogeneous medium. Maxwell model is good for low solid concentrations. Relative thermal conductivity enhancement (ratio of the effective thermal conductivity k_{eff} of nanofluid to base fluid k_f) is,

$$k_{eff} / k_f = \frac{k_p + 2k_f + 2\phi(k_p - k_f)}{k_p + 2k_f - \phi(k_p - k_f)} \quad (2.1)$$

where ϕ is the particle volume fraction of the suspension, k_p is the thermal conductivity of the particle. According to Maxwell model the effective thermal conductivity of suspensions depending on the thermal conductivity of spherical particles, base liquid and the volume fraction of solid particles.

Bruggeman (1935) proposed a model to analyze the interactions among randomly distributed particles by using the mean field approach.

$$k_{eff} = \frac{1}{4} [(3\phi - 1)k_p + (2 - 3\phi)k_f] + \frac{k_f}{4} \sqrt{\Delta} \quad (2.2)$$

where,

$$\Delta = \left[(3\phi - 1)^2 (k_p / k_f)^2 + (2 - 3\phi)^2 + 2(2 + 9\phi - 9\phi^2) (k_p / k_f) \right] \quad (2.3)$$

When Maxwell model fails to provide a good match with experimental results for higher concentration of inclusions, Bruggeman model can sufficiently be used.

Hamilton & Crosser (1962) modified Maxwell's model to determine the effective thermal conductivity of non-spherical particles by applying a shape factor n . The formula yields,

$$k_{eff} / k_f = \frac{k_p + (n-1)k_f - (n-1)\phi(k_f - k_p)}{k_p + (n-1)k_f + \phi(k_f - k_p)} \quad (2.4)$$

where $n=3/\psi$ and ψ is the sphericity, defined by the ratio of the surface area of a sphere, having a volume equal to that of the particle, to the surface area of the particle.

Since these conventional models were found to be unable to predict the experimental observations described above, Wang et al. (1999) concluded that any new effective thermal conductivity model of nanofluids should include the effects of microscopic motion and chain structure of nanoparticles.

Keblinski, Phillpot, Choi & Eastman (2002) assessed various mechanisms for the anomalous enhancement: (1)Brownian motion of the particles, (2)molecular-level layering of the liquid at the liquid/particle interface, (3)the nature of heat transport in the nanoparticles, and (4)the effects of nanoparticle clustering.

2.4.1 Brownian Motion of Particles

Brownian motion was investigated by many groups as a possible enhancement reason of thermal conductivity of nanofluids. Mainly there are two types theoretical models, one is based on translational Brownian motion of the nanoparticles(Bhattacharya et al., 2004), and the other based on microconvection caused by the Brownian motion of the nanoparticles(Prasher, Bhattacharya & Phelan, 2005; Jang & Choi, 2004). Jang & Choi (2004) devised a theoretical model that includes four modes of energy transport; the collision between basefluid molecules,

the thermal diffusion of nanoparticles in the fluid, the collision between nanoparticles due to Brownian motion, and the thermal interactions of dynamic nanoparticles with base fluid molecules.

$$k_{eff} / k_f = (1 - \phi) + \frac{k_p}{k_f} \phi + 3C \frac{d_f}{d_p} \phi \text{Re}_{d_p}^2 \text{Pr} \quad (2.5)$$

where Re_{d_p} is the Reynolds number defined by $\text{Re}_{d_p} = (C_{RM} d_p) / \nu$, C is a proportional constant, C_{RM} is the random motion velocity of nanoparticles, ν is the dynamic viscosity of the base fluid, Pr is the Prandtl number, d_f and d_p are the diameter of the base fluid molecule and particle. For typical nanofluids, the order of the Reynolds number and the Prandtl numbers are 1 and 10, respectively.

However Keblinski et al. (2002) demonstrated that thermal diffusion is much faster than Brownian diffusion even within the limits of extremely small particles and they have concluded this with support of the molecular dynamics simulations (MDS). Evans et al. (2006) confirmed Keblinski et al. (2002), by showing that the hydrodynamics effects associated with Brownian motion have only a minor effect on thermal conductivity of nanofluid. On the other hand Sarkar & Selvam (2007) showed that by the presence of nanoparticles, heat conduction enhances mostly due to the increased movement of liquid atoms.

2.4.2 Molecular-level Layering of the Liquid at the Liquid/Particle Interface

Yu et al. (2000), experimentally showed that in particle-fluid mixtures the liquid molecules close to a particle surface form layered structures and behave much like a solid. Therefore, the atomic structure of such liquid layer is significantly more ordered than that of the bulk liquid. Some groups (Xue, 2003; Yu & Choi, 2004; Wang, Zhou & Peng, 2003; Xie, Fujii & Zhang, 2005; Ren, Xie & Cai, 2005; Tillman & Hill, 2007) assumed a solid-like layer of thickness with few nanometers that surrounding the nanoparticle as a shell and they proposed that the existence of solid-like nanolayers between nanoparticles and the fluid may play a key role in the enhancement of thermal conductivity.

Yu & Choi (2004), derived a model for the effective thermal conductivity of nanofluid by assuming that there is no agglomeration by nanoparticles in nanofluids. They assumed that the nanolayer surrounding each particle could combine with the particle to form an equivalent particle and obtained the equivalent thermal conductivity k_{pe} of equivalent particles as follows,

$$k_{pe} = \frac{[2(1-\gamma) + (1+\beta)^3(1+2\gamma)\gamma]}{-(1-\gamma) + (1+\beta)^3(1+2\gamma)} k_p \quad (2.6)$$

where $\gamma = k_{\text{layer}}/k_p$, is the ratio of the nanolayer thermal conductivity to particle conductivity, and $\beta = h/r$ is the ratio of nanolayer thickness to the original particle radius.

$$k_{eff} / k_f = \frac{k_{pe} + 2k_f + 2\phi(k_{pe} - k_f)(1-\beta)^3}{k_{pe} + 2k_f - \phi(k_{pe} - k_f)(1+\beta)^3} \quad (2.7)$$

Xie et al. (2005), derived an expression for calculating enhanced thermal conductivity of nanofluid by considering the effects of nanolayer thickness, nanoparticle size, volume fraction, and thermal conductivity ratio of particle to fluid. The expression is:

$$k_{eff} / k_f = \left(1 + 3\Theta\phi_T + \frac{3\Theta^2\phi_T^2}{1-\Theta\phi_T} \right) \quad (2.8)$$

with

$$\Theta = \frac{\beta_{lf} [(1+\gamma)^3 - \beta_{pl} / \beta_{fl}]}{(1+\gamma)^3 + 2\beta_{lf}\beta_{pl}} \quad (2.9)$$

where

$$\beta_{lf} = \frac{k_l - k_f}{k_l + 2k_f}, \quad \beta_{pl} = \frac{k_p - k_l}{k_p + 2k_l}, \quad \beta_{fl} = \frac{k_f - k_l}{k_f + 2k_l} \quad (2.10)$$

and $\gamma = \delta/r_p$ is the thickness ratio of nano-layer and nanoparticle. k_l is the thermal conductivity of nanolayer and ϕ_T is the modified total volume fraction of the original nanoparticle and nano-layer, $\phi_T = \phi (1 + \gamma)^3$.

However, by using molecular dynamics simulations and simple liquid–solid interfaces, Xue et al. (2004) have demonstrated that the layering of the liquid atoms at the liquid–solid interface does not have any significant effect on thermal transport properties.

2.4.3 Nature of Heat Transport in Nanoparticles

When the size of the nanoparticles in a nanofluid becomes smaller than the phonon mean free path, phonon can not diffuse across the particles, but must move ballistically (Keblinski et al., 2002). Agop, Stan, Toma & Rusu (2007), analyzed the heat transfer in nanofluids by using the scale relativity theory, assuming that in nanofluids the heat moves in a ballistic manner. So far not much effort has been put into for heat transport in nanofluids by means of ballistic.

2.4.4 Effects of Nanoparticle Clustering

Keblinski et al. (2002), illustrated the effect of clustering by considering the effective volume of a cluster is much larger than the volume of the particles due to the lower packing fraction of the cluster (ratio of the volume of the solid particles in the cluster to the total volume of the cluster). Some more studies emphasized that nanoparticle aggregation plays a critical role in the thermal transport of nanofluids (Wang et al., 2003; Xuan, Li & Hu, 2003; Kwak & Kim, 2005; Hong et al., 2006; Prasher et al., 2006; Evans et al., 2008). Wang et al. (2003), proposed a model based on the effective medium approximation and the fractal theory for the description of nanoparticle cluster and its radial distribution also by taking consideration of size effect and surface adsorption of the particles. Xuan et al. (2003) derived a theoretical model by considering the physical properties of both the base liquid and the nanoparticles as well as the structure of the nanoparticles and

aggregation. Hong et al. (2006), analysed the effect of aggregation and sonication on the thermal properties of Fe based nanofluids and showed that the thermal conductivity increases with sonication time and reduced cluster size. Prasher et al. (2006) and Evans et al. (2008) have demonstrated that enhancement of thermal conductivity is a function of nanoparticle aggregation. According to this mechanism, there is an optimized aggregation structure for attaining maximum thermal conductivity. By using three-level homogenization theory, validated by Monte Carlo simulation of heat conduction on model fractal aggregates, they have demonstrated based purely on thermal conduction physics that the thermal conductivity of nanofluids and nanocomposites can be significantly enhanced as a result of aggregation of the nanoparticles. The conductivity enhancement due to aggregation is also a strong function of the chemical dimension of the aggregates and the radius of gyration of the aggregates.

In addition to these models there are many other models, but no single model explains the effective thermal conductivity in all cases. Besides the thermal conductivities of the base fluid and nanoparticles and the volume fraction of the particles, there are many other factors influencing the effective thermal conductivity of the nanofluids. Some of these factors are: the size and shape of nanoparticles, the agglomeration of particle, the mode of preparation of nanofluids, the degree of purity of the particles, surface resistance between the particles and the fluid. Some of these factors may not be predicted adequately and may be changing with time. This situation emphasizes the importance of having experimental results for each special nanofluid produced.

2.5 Viscosity of Nanofluids

Masuda et al. (1993) were the first who measured the viscosity of suspensions of dispersed nanoparticles in water. They found that TiO₂ nanoparticles at a volumetric loading of 4.3% water increased the viscosity of water by 60%.

Pak & Cho (1998), measured the viscosity of Al_2O_3 -water and TiO_2 -water nanofluids by using a Brookfield rotating viscometer with cone and plate geometry. The volume concentration was varied 1% to 10%. The relative viscosity for the dispersed fluid with Al_2O_3 particles was approximately 200, while it was approximately 3 for dispersed fluids with TiO_2 particles. These viscosity results were significantly larger than the predictions from the classical theory of suspension rheology.

Das, Putra & Roetzel (2003) measured the viscosity of Al_2O_3 -water nanofluids by a rotating disc method. Their results showed a similar trend of increase of relative viscosity with increased particle concentration. Also their experiments conducted against shear rate indicated that nanofluid behavior is Newtonian.

Prasher et al. (2006) used a controlled stress rheometer, with a double-gap fixture for measuring the viscosity of Al_2O_3 -propylene glycol nanofluid. They concluded that the nanofluids are Newtonian and relative viscosity of Al_2O_3 -propylene glycol nanofluids is independent of temperature.

Namburu, Kulkarni, Dandekar & Das (2007) investigated the viscosity of SiO_2 nanoparticles suspended in 60:40 (by weight) ethylene glycol – water mixture, by using Brookfield rotating viscometer. They found that at lower temperatures it shows non-Newtonian behaviour, whereas at high temperatures it is Newtonian.

Murshed et al. (2008b) measured the viscosity of TiO_2 -water nanofluid by controlled rate rheometer. They found almost 80% increase in viscosity at particle volumetric loading of 5%.

All published reports show that the viscosity of nanofluids is increased dramatically and can not be predicted by classical models such as Einstein (1956) or Nielsen (1970). According to these classical models the effective viscosity depends on the viscosity of base fluid and on the concentrations of the particles, whereas the experimental studies show that the particle diameter, the kind of particle and the

temperature can affect the effective viscosity of nanofluids (Masoumi, Sohrabi, & Behzadmehr, 2009)

Recently, an analytical model for calculation of effective viscosity of nanofluids was presented by Masoumi et al. (2009). Their model determines the effective viscosity of nanofluids as a function of temperature, the mean nanoparticle diameter, the nanoparticle volume fraction, the nanoparticle density and the base fluid physical properties.

It is clear that the gain from thermal conductivity might be offset by the increase of viscosity. For objective evaluation of the application of nanofluids, in addition to the thermal conductivity, the viscosity should be paid more attention.

CHAPTER THREE
3 ω METHOD FOR MEASURING
THERMAL CONDUCTIVITY OF (NANO)FLUIDS

3.1 Introduction

Steady state methods to measure thermal conductivity are subject to the difficulty to establish a really stationary temperature gradient in the sample. For fluids there is an additional difficulty in preventing natural convection phenomena. There are mainly two non-stationary methods to measure thermophysical properties: the transient hot wire technique (Nagasaka & Nagashima, 1981) and the temperature oscillation technique (Bhattacharya et al., 2006). The study of nanofluids is usually performed with combined flow and (transient) heat-transfer instruments (Kostic, 2006) and reports on the use of ac thermal methods are scarce (Das, Putra, Thiesen & Roetzel, 2003).

A modulated hot wire k measurement of liquids is reported by (Powell, 1991). A Wollaston wire thermal probe designed for microthermal analysis was used with ac excitation current for the evaluation of k when completely immersed in different pure liquids (Buzin, Kamasa, Pyda & Wunderlich, 2002). By using 3ω method in conjunction with a thin film metal strip deposited on a solid substrate, the k value of the latter (Cahill, 1990) or the thermal effusivity of a glass-forming liquid in contact with this sensor (Birge & Nagel, 1987) were determined. A comprehensive discussion of 1ω , 2ω , and 3ω methods is contained in reference (Dames & Chen, 2005).

We report here thermal conductivity k measurement of nanofluids in a configuration using an ac excited hot wire immersed in a stationary fluid, combined with lock-in detection of the third harmonic (3ω method).

3.2 Theoretical Background

3.2.1 3- ω Signal Generation

We consider a thermal probe (ThP) consisting of a metallic wire of length $2l$ and radius r immersed in a liquid sample. The sample and probe thermophysical properties are the density ρ , the specific heat c and the thermal conductivity k , with the respective subscripts (s) and (p). The wire is excited by ac current $I(t) = I_0 \cos(\omega t)$. We use the notation 2ω and $2f$ for the second harmonic of the modulated excitation current since the thermal phenomena are modulated at this frequency. The temperature $\theta(f, t)$ has a 2ω component, proportional to the power $I^2(t) R_0$. We assume that due to its large thermal conductivity, the wire is thermally thin in the radial direction so that $\theta(f, t)$ is uniform over its cross section. The electrical resistance of the wire $R(t)$ (with r_{el} the temperature coefficient of the resistivity ρ_{el}) oscillates also at 2ω :

$$R(t) = R_0 [1 + r_{el} \theta_{2\omega} \cos(2\omega t - \varphi)] \quad (3.1)$$

The voltage across the wire reads:

$$V(t) = I(t)R(t) = I_0 R_0 \{ \cos(\omega t) + (1/2) r_{el} \theta_{2\omega} [\cos(\omega t - \varphi) + \cos(3\omega t - \varphi)] \} \quad (3.2)$$

The term depending on 3ω is generated by the mixing of excitation current at ω with the resistance change at 2ω :

$$V_{3\omega}(f) = \frac{I_0 R_0}{2} r_{el} \theta_{2\omega} \quad (3.3)$$

At low frequency (up to 1 kHz for the used ThP), the heat stored in the heat capacity of the wire is negligible and one may consider that the input electrical power is

completely dissipated by lateral conduction to the fluid. Then the temperature amplitude $\theta_{2\omega}$ is given by:

$$\theta_{2\omega} = P_{2\omega} \frac{Z_s}{2} = \frac{I_0^2 \rho_{el} (2l)}{2\pi r^2} \frac{Z_s}{2} \quad (3.4)$$

where the power amplitude at the second harmonic is half that given by $I_0^2 R_0$. Z_s [K/W] is the thermal impedance of the interface between the (half-length) wire and the liquid sample. It is convenient to use dimensionless impedance instead that we shall refer to as the F factor (Chirtoc & Henry, 2008):

$$F = \frac{Z_s}{Z_p} = \frac{z_s / 2\pi r l}{l / (\pi r^2 k_p)} = \frac{k_p r}{2l^2} z_s \quad (3.5)$$

where z_s [m² K/W] is the specific thermal impedance of the interface. Z_p represents the thermal resistance of the half-length wire in the axial direction, considering the end supports as infinite heat sinks. If $F \ll 1$ the wire is thermally long and heat loss to end supports can be neglected.

With equations (3.4) and (3.5), equation (3.3) becomes in terms of effective values:

$$V_{3\omega eff}(f) = \left(\frac{I_{eff} l}{\pi r^2} \right)^3 C_M F(f) \quad (3.6)$$

Here $C_M = \rho_{el}^2 r_{el} / k_p$ is a figure of merit of the wire material (Chirtoc et al., 2004). Equation (3.6) shows the way to normalize the measured 3ω signal in terms of F factor, which can be regarded also as a reduced amplitude.

3.2.2 Interface Thermal Impedance

The temperature increase $\theta(r,f)$ generated by a line heat source in an infinite and homogeneous medium is given by the ac solution in cylindrical geometry. For periodic excitation with power amplitude per unit length $P_{2\omega}/l$ [W/m], the temperature amplitude is given by (Carslaw & Jeager, 1959):

$$\theta(r, f) = \frac{P_{2\omega}/l}{2\pi k_s} K_0(\sigma_s r) \quad (3.7)$$

where K_0 is the zeroth-order modified Bessel function. The complex argument is $\sigma_s r = (1+i)r/\mu_s$ with $\mu_s = [\alpha_s \pi^{-1}(2f)^{-1}]^{1/2}$ the thermal diffusion length in the medium at frequency $2f$ and $\alpha_s = k/\rho c$ the thermal diffusivity. We use equation (3.7) to describe the temperature at the wire-sample interface. For $r/\mu_s \ll 1$ (low frequency) by keeping the first term in series development of $K_0(\sigma_s r)$, one obtains:

$$\theta_{2\omega} = -\frac{P_{2\omega}}{2\pi k_s l} \left(\gamma + \ln \frac{\sigma_s r}{2} \right) \quad (3.8)$$

where $\gamma = 0.5772$ is the Euler constant, or by rearranging the terms (Cahill, 1990):

$$\theta_{2\omega} = \frac{P_{2\omega}}{2\pi k_s l} \left(\ln \frac{\mu_s}{1.2594 r} - i \frac{\pi}{4} \right) \quad (3.9)$$

From equation (3.9) the specific thermal impedance is obtained as $z_s = 2\pi r l \theta_{2\omega} / P_{2\omega}$ and finally the F factor becomes:

$$F = \frac{k_p r^2}{2k_s l^2} \left(\ln \frac{\mu_s}{1.2594 r} - i \frac{\pi}{4} \right) \quad (3.10)$$

One can see that the F factor (and the 3ω signal magnitude) is proportional to the reciprocal of the sample thermal conductivity k_s and it has a weaker dependence on the thermal diffusivity α_s and on f .

3.2.3 Data Reduction Method

The real part of equation (3.10) has been used for the determination of thermal conductivity of solids (Dames & Chen, 2005). The sensor consisted of a thin film metal strip deposited on the surface of a solid and could not be transferred onto a reference material. Therefore the only possibility was to determine k_s from the slope of $\text{Re}(F)$ vs. $\log(f)$. In contrast, our thermal probe is independent of the sample and allows multiple use as well as calibration measurements with a reference sample. In this work we are concerned with the measurement of thermal properties of water-based nanofluids, relative to pure water (subscript w). We adopted the following data reduction scheme requiring, in principle, a single frequency measurement. From equation (3.10) one has:

$$\frac{k_s}{k_w} = \frac{\text{Im}(F_w)}{\text{Im}(F_s)} \quad (3.11)$$

with no influence from α_s or from frequency. There is an optimum frequency range such that $r/\mu_s < 1$ in which equation (3.11) yields low noise and stable results as a function of frequency.

3.3 Experimental

The thermal probe (ThP) (Figure 3.1) was made of 40 μm in diameter and $2l = 19.0$ mm long Ni wire having the following properties: $\rho_p = 8900$ kg m^{-3} , $c_p = 444$ $\text{J kg}^{-1} \text{K}^{-1}$, $k_p = 90.9$ $\text{W m}^{-1} \text{K}^{-1}$, $\rho_{el} = 6.91 \times 10^{-8}$ Ωm , $r_{el} = 5.19 \times 10^{-3}$ K^{-1} , $C_M = 0.272 \times 10^{-18}$ $\Omega^2 \text{m}^3 \text{W}^{-1}$.

The first term in equation (3.2) is dominant and must be cancelled by a Wheatstone bridge arrangement. The selection of the 3rd harmonic from the differential signal across the bridge is performed by a Stanford SR850 lock-in amplifier tuned to this harmonic (Figure 3.2 and 3.3). A measurement with automatic frequency scan and 1 s time constant takes 16 s per point. With an exciting current of $I_{eff} = 0.17$ A, the temperature oscillation amplitude $\theta_{2\omega}$ in water was 1.25 K, generating a 3ω signal in the 0.1 mV range. The liquid sample volume was typically 100 ml, but the minimum volume for equation (3.8) to apply is that of a liquid cylinder centered on the wire and having a radius equal to about $3\mu_s$. At $2f = 1$ Hz, this amounts to 25 μ l.

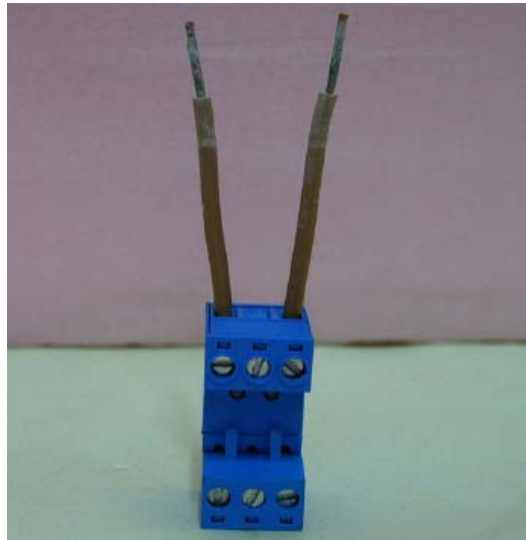


Figure 3.1. Thermal probe

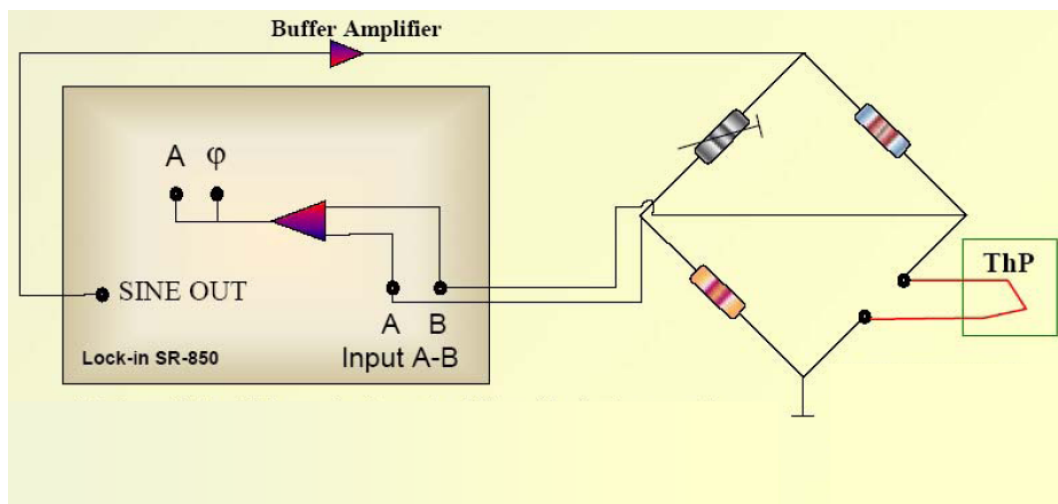


Figure 3.2 Schematic diagram of 3ω experimental set-up.

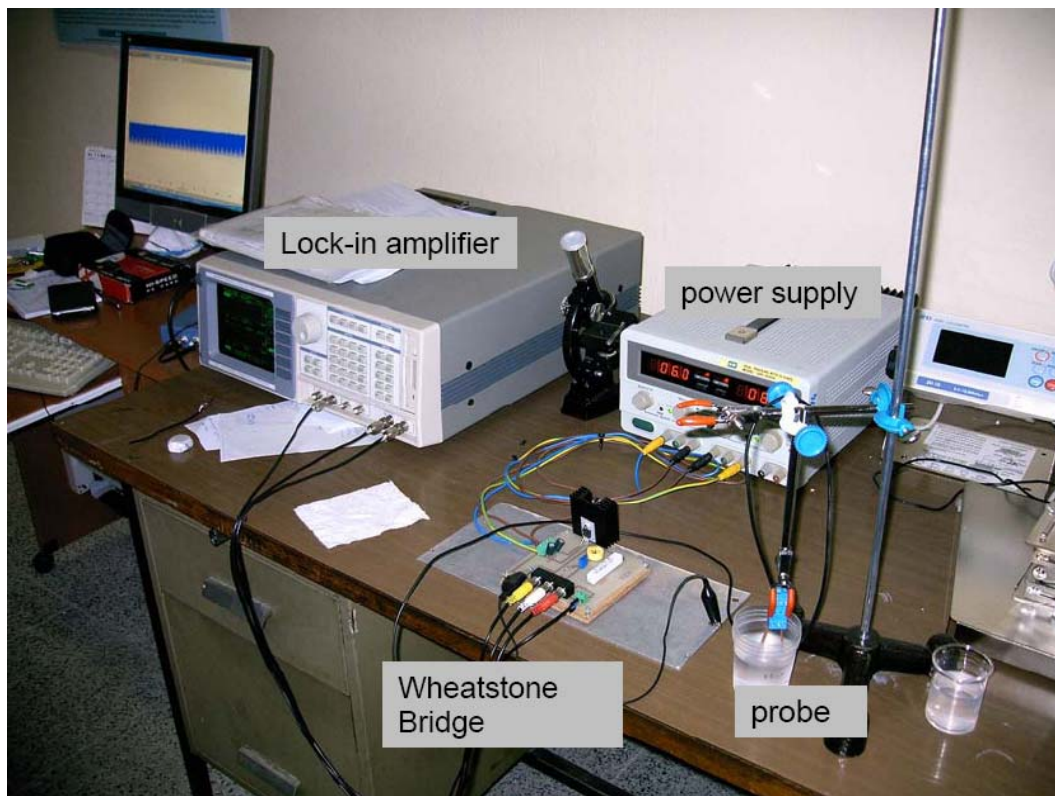


Figure 3.3 Experimental set-up for 3ω method consisting of thermal probe (ThP), Wheatstone bridge and lock-in amplifier.

3.4 Results and Discussion

Figure 3.4 shows a typical measurement on water (points), expressed in terms of reduced amplitude (F factor) by evaluating the constants in equation (3.6). The curves represent theoretical simulations with equation (3.10). It is obvious that the imaginary part cannot be neglected. The agreement between theory and experiment is good below 1 Hz and justifies the assumptions of the theoretical section, including the condition $F \ll 1$. The deviation from the theoretical curves is apparent as the frequency increases above 1 Hz, and is more pronounced in the signal phase. This is because at $2f = 100$ Hz, $r/\mu_w \approx 1$. In theory, the asymptotic low frequency phase limit is 0° , but the lock-in has a mixing phase shift of 180° . The relative conductivities were computed using equation (3.11).

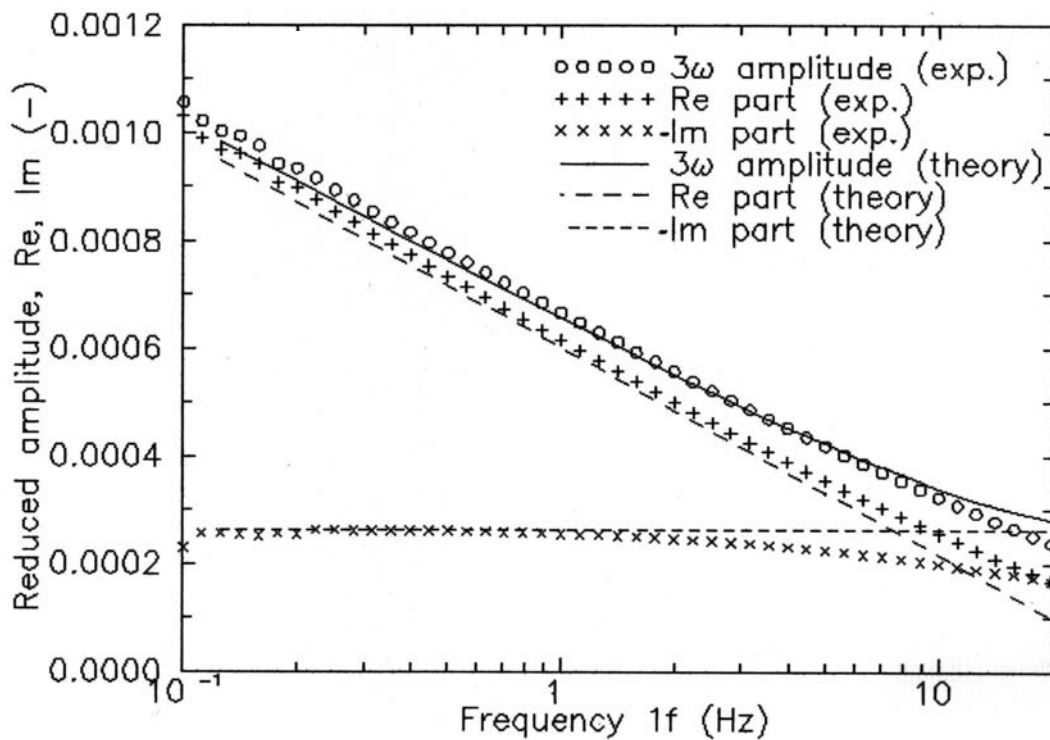


Figure 3.4 Experimental results of 3ω amplitude and its components for water (points). The reduced amplitude (F factor) was determined from Eq. (3.6) in the conditions of the experiment. The curves are simulations with Eq. (3.10).

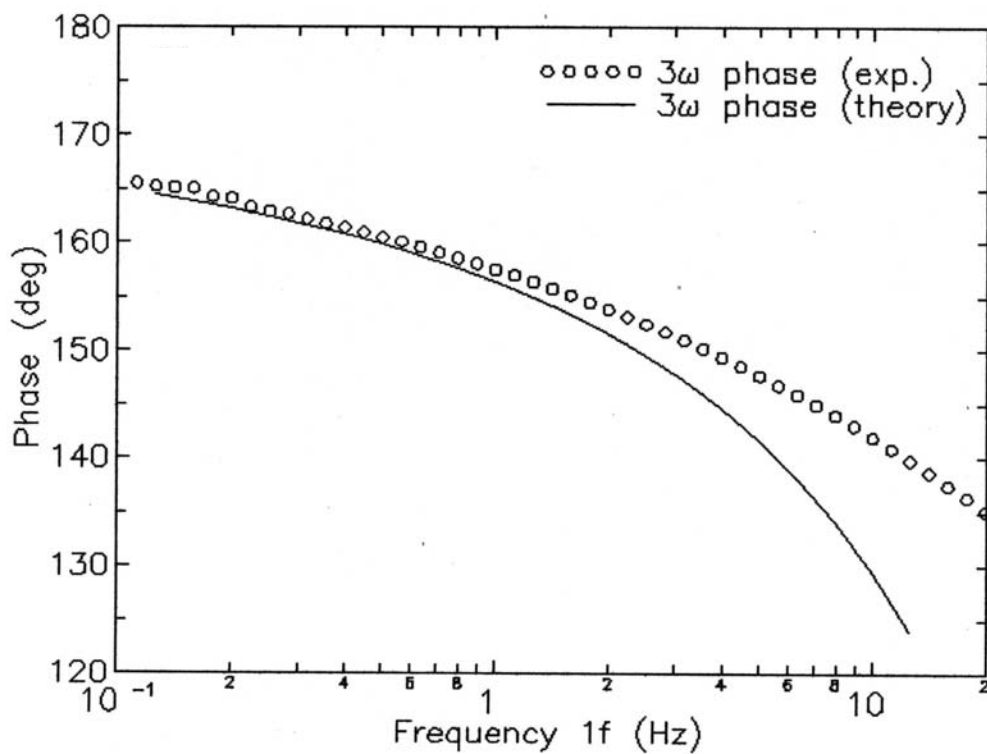


Figure 3.5 Experimental results of 3ω phase for water (points). The curve is simulation with Eq. (3.10).

Ethylene glycol, methanol and ethanol were chosen for the calibration of the system. Table 3.1 presents the comparison of the measured thermal conductivity and reference values (Lide, 2007) at three temperatures. Each thermal conductivity measurement was repeated five times. The error for the reference data is reported to be less than 2%.

Table 3.1 Validation of the 3ω method with ethylene glycol, ethanol and methanol

Temperature	25°C			50°C			75°C		
	k (W/mK)		%	k (W/mK)		%	k (W/mK)		%
Sample	Exp	Ref*	Error	Exp	Ref*	Error	Exp	Ref*	Error
Ethylene Glycol	0.252	0.254	0.79	0.255	0.258	1.16	0.257	0.261	1.53
Ethanol	0.165	0.167	1.19	0.158	0.160	1.88	0.150	0.153	1.96
Methanol	0.200	0.202	0.99	0.192	0.195	1.53	0.186	0.189	1.58

*(Lide, 2007)

3.5 Conclusion

We built a hot wire sensor and we developed a data reduction method for measurement of thermal conductivity k of small quantity of liquid samples, typically 25 μ l. The requirements for the validity of the theoretical analysis are easily fulfilled in practice. There are no constraints on sample geometry except the minimum sample volume. The thermal probe plays the role of excitation source and temperature sensor in the same time. It is compact, reusable and low cost, and it is compatible with temperature-dependent measurements. Due to ac modulation and lock-in signal processing, the long-term reproducibility of absolute value is 0.3%, in the case of relative measurements, the resolution is 0.1% in k . These values make the device very attractive for accurate thermophysical investigations of (nano)fluids.

CHAPTER FOUR

PROCESSING OF NANOFLUIDS

4.1 Introduction

Production of the nanofluids is the most important step for conducting the enhanced thermal properties. Produced nanofluids must be long term stable. There are two common methods of producing nanofluids. One is single-step method and the other is two-step method. Single-step method is a process simultaneously makes and disperses the nanoparticles in the base fluid. In a two-step method, firstly the particles are produced independently and this step is followed by particles dispersion in the liquid. The major advantage of the two-step technique is the possibility to use commercially available nanoparticles, this method provides an economical way to produce nanofluids. But, the major drawback is the tendency of the particles to agglomerate due to attractive van der Waals forces between nanoparticles; then, the agglomerations of particles tend to quickly settle out of liquids. This problem is overcome by using ultrasonic vibration, to break down the agglomerations and homogenize the mixture. Figure 4.1 shows Al_2O_3 -water nanofluids with and without homogenization process. As we can easily see without homogenization nanoparticles are settled.



Figure 4.1 Comparative samples showing the alumina nanofluids without and with sedimentation.

We have used two-step method for this study. This chapter describes the preparation process and stability of our nanofluids.

4.2 Properties of particles and basefluids

The nanoparticles used in this work were SiO₂, TiO₂ and Al₂O₃ with average particle diameters 12, 21 and 25 nm, respectively. SiO₂ (AEROSIL[®] 200V) and TiO₂ (AEROXIDE[®] P25) particles were supplied from Degussa (Germany) and Al₂O₃ was supplied from NanoAmor (USA). De-ionized water and ethylene glycol (99.5% purity, Carlo Erba) were used as the base-fluids. The volume fraction of particles (Table 4.1) was calculated from weight of dry powder using the true density (Table 4.2) supplied from manufacturer and the density of liquids. In equation 4.1 ϕ_V , represents the volume fraction of the particles where ρ_W and ρ_P are density of the fluid and particles respectively. ϕ_W is the mass fraction of the particles dispersed in the nanofluids.

$$\phi_V = \frac{\phi_W \rho_W}{\rho_P + \phi_W \rho_W - \phi_W \rho_P} \quad (4.1)$$

Table 4.1 Volumetric particle concentrations of produced nanofluids

	Nanoparticles				
	SiO ₂	TiO ₂	Al ₂ O ₃	Al ₂ O ₃	Al ₂ O ₃
Manufacturer	Degussa	Degussa	NanoAmor	NanoAmor	NanoAmor
Average particle diameter (nm)	12	21	25	25	25
Particle volumetric concentrations (%)	0.45, 1.85, 4.0	0.2, 1.0, 2.0, 3.0	0.5, 1.0, 1.5 2.0, 3.0, 4.0, 5.0	1.0* (at 4 different mass ratio of SDBS/Al ₂ O ₃)	0.5, 1.0, 2.0, 3.0, 4.0, 5.0
Base-fluid	water	water	water	water + SDBS*	ethylene glycol

* Sodium dodecylbenzenesulfonate(SDBS) was used as a surfactant for Al₂O₃ –water nanofluid. We have investigated the effect of the different concentrations of SDBS on thermal conductivity and viscosity of nanofluids. We have prepared Al₂O₃ –water nanofluids with 1% volumetric concentration of Al₂O₃ particles and with varying mass ratio of SDBS/Al₂O₃ at 0.1, 0.25, 0.5 and 1.0.

Table 4.2 Density and thermal conductivity values of particles and base-fluids

Properties	Materials				
	SiO ₂	TiO ₂	Al ₂ O ₃	Water	Ethylene glycol
Density (kg/m ³)	2220	3800	3700	1000	1106
Thermal conductivity (W/mK)	1.38	10	46	0.613	0.252

4.3 Preparation of nanofluids

Sensitive mass balance (PRECISA XB220A) with accuracy 0.1 mg was used during the preparation of nanofluids (Figure 4.2). After the particles were added into the base-fluid, the suspensions were ultrasonicated by Misonix Sonicator 3000. Operating frequency and the maximum power of the equipment is 20 kHz and 600 Watts, respectively (Figure 4.3). In our case all the ultrasonication processes were carried out by ½” tip horn with 110-120 watts effective power at the tip of the horn. We provided a cold bath surrounding the sample flask, because during ultrasonication with the increasing temperature of the sample, the effective power at the tip of the horn is decreasing. For the 50 ml quantity, all the samples were applied to 110-120 Watts (2.2 – 2.4 W/mL) through 30 minutes.



Figure 4.2 Measuring the mass of the particles and liquids by mass balance.

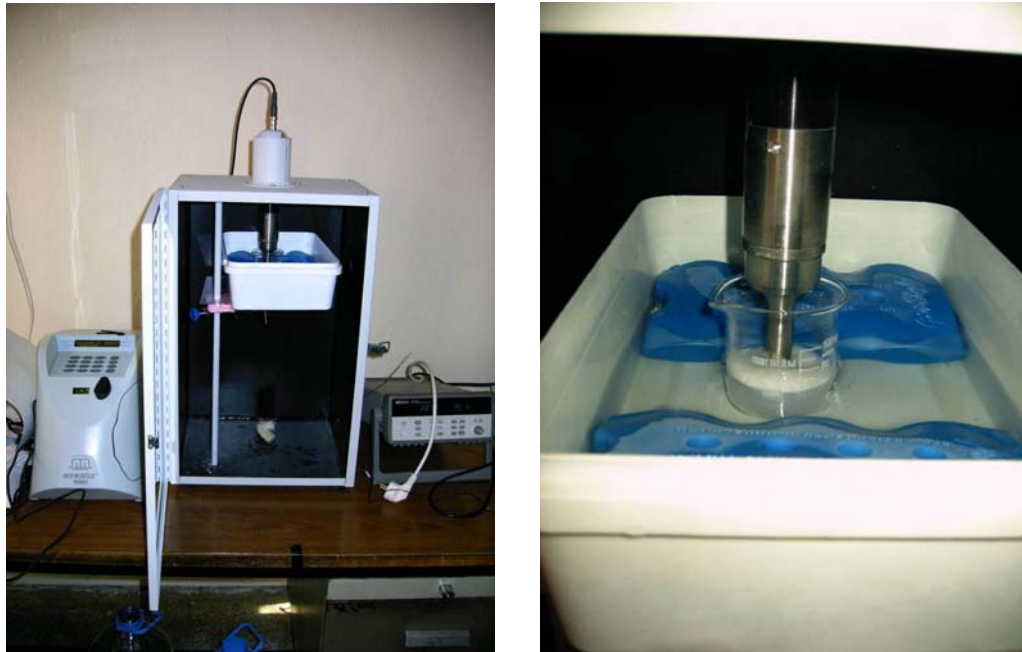


Figure 4.3 Sonication of the nanofluids by Misonix 3000.



Figure 4.4 Photograph showing a set of produced nanofluids with volume fraction of alumina from 0.5 to 5 vol %.

4.4 Zeta potential of nanofluids

For the industrial application of nanofluids, stable suspension of nanoparticles and uniform dispersion is the key factor. Zeta potential is herein an important parameter that reflects the colloid behavior of the particles. It is known from the literature (Lee et al., 2008) that a suspension with zeta potential below 20 mV has limited stability, below 5 mV it is accepted as an aggregation, and above 30 mV it is physically stable. Zeta potential of SiO_2 – water and TiO_2 – water nanofluids were measured by Colloidal-Dynamics Acousto Sizer II. For Al_2O_3 – water and Al_2O_3 – EG nanofluids Malvern Zetasizer 3000 HSA was used to measure zeta potential.

Measured zeta potential values of SiO_2 – water, TiO_2 – water, Al_2O_3 – water and Al_2O_3 – EG nanofluids were 30 mV, 38 mV, 55 mV and 69 mV, respectively. This shows that all our samples are physically stable.

CHAPTER FIVE

THERMAL CONDUCTIVITY OF NANOFLUIDS

5.1 Introduction

After the pioneering work of Choi (1995), nanofluids become a new class of heat transfer fluids. Their potential benefits and applications in many industries from electronics to transportation have attracted great interest from many researchers both experimentally and theoretically.

Published results show an enhancement in the thermal conductivity of nanofluids, in a wide range even for the same host fluid and same nominal size or composition of the additives. Since this enhancement can not be explained with the existing classical effective thermal-conductivity models such as the Maxwell (1881) or Hamilton – Crosser (1962) models, this also motivates a wide range of theoretical approaches for modeling these thermal phenomena. Reported results show that particle volume concentration, particle material, particle size, particle shape, base fluid material, temperature, additive, and acidity play an important role in enhancement of the thermal conductivity of nanofluids.

The effect of the fluid temperature on the effective thermal conductivity of nanoparticle suspensions was first presented by (Masuda, Ebata, Teramae & Hishinuma, 1993). They reported that for water-based nanofluids, consisting of SiO₂ and TiO₂ nanoparticles, the thermal conductivity was not much more temperature dependent than that of the base fluid. Contrary to this result, Das et al. (2003) observed a two-to-four fold increase in the thermal conductivity of nanofluids, containing Al₂O₃ and CuO nanoparticles in water, over a temperature range of 21 °C to 51 °C. Several groups (Patel et al., 2003; Wen & Ding, 2004; Chon & Kihm, 2005; Li & Peterson, 2006; Wang, Tang, Liu, Zheng & Araki, 2007; Murshed, Leong & Yang, 2008b; Mintsa, Roy, Nguyen & Doucet, 2009) reported studies with different nanofluids, which support the result of Das et al., (2003). For the temperature dependence of the relative thermal conductivity (ratio of effective

thermal conductivity of nanofluids to thermal conductivity of base fluid), although a major group of publications showed an increase with respect to temperature, some of the other groups observed a moderate enhancement or temperature independence (Masuda et al., 1993; Venerus, Kabadi, Lee & Perez-Luna, 2006; Zhang, Gu & Fujii, 2006; Yang & Han, 2006; Timofeeva et al., 2007).

In this chapter we present experimental measurements of the effective thermal conductivity of nanofluids by using the 3ω method at different temperatures. We compare our experimental results with those in the literature also with effective thermal conductivity models.

5.2 Materials

We have prepared several nanofluids with varying particle volumetric concentrations such as SiO₂ – water (0.45, 1.85, 4.0% vol.), TiO₂ – water (0.2 to 3.0% vol.), Al₂O₃ – water (0.5 to 5.0% vol.) and Al₂O₃ – EG (0.5 to 5.0% vol.), Al₂O₃ – water+SDBS (1.0 % vol.). In chapter 4 we have given the properties of the materials and preparation process of the nanofluids.

5.3 Results and Discussion

5.3.1 Effect of Ultrasonication Time

In order to decide on a sonication time to be used in the preparation of nanofluids, we applied different sonication times for 1 % by volume TiO₂-water nanofluids and measured the relative thermal conductivity. From Figure 5.1, it may be seen that sonication time has practically no effect on thermal conductivity after 30 minutes, therefore we decided to use 30 minutes of sonication time. This duration looks similar with Hwang et al. (2008) and Zhu et al. (2009) but much shorter than 3 hours (Li et al., 2006 and Ju et al., 2008) or 8 – 12 hours (Das et al., 2003; Kwak et al., 2005 and Murshed et al., 2006).

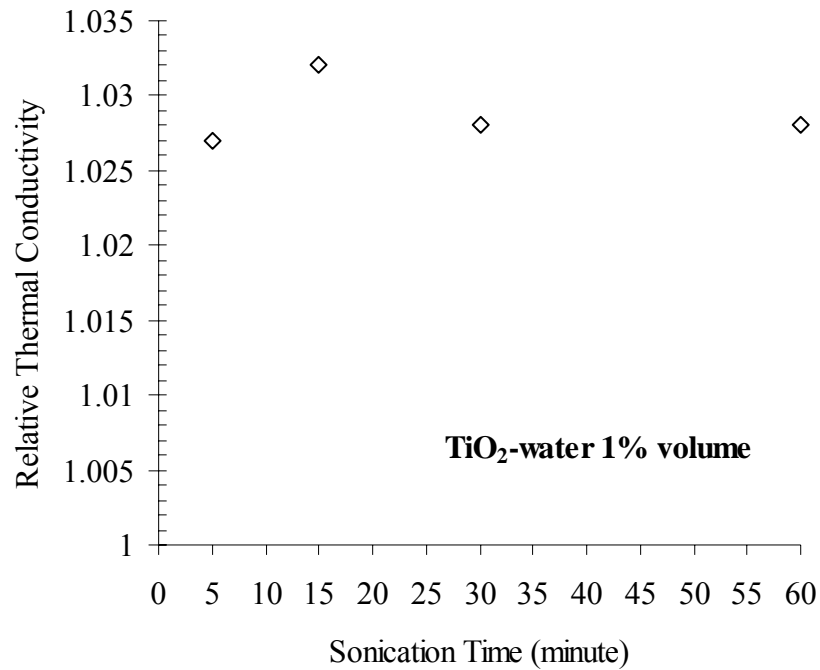


Figure 5.1 Relative thermal conductivity of TiO₂-water nanofluid (1% volume particle concentration), as a function of the sonication time.

5.3.2 Effect of Volume Fraction and Temperature

5.3.2.1 SiO₂ – water Nanofluids

The effective thermal conductivity of SiO₂-water nanofluids with concentration 0.45, 1.85, 4.0 vol.% were measured at 20°C. The comparison of our results for the thermal conductivity enhancement of SiO₂-water nanofluids with the data of other groups from the literature (Kang et al. 2006; Hwang et al. 2006 and Wang et al. 2007) is given in Table 5.1a and b. For the maximum particle volume fraction (4 %), enhancement in the thermal conductivity is only 2.2 % for our results, on the other hand for the same volume fraction Kang et al. (2006) found 5 % enhancement. By taking the ratio of thermal conductivity enhancement to the nanoparticle volume fraction, one obtains the *Reduced Thermal Conductivity Enhancement*. Our data for reduced thermal conductivity enhancement is in the range of 0.44 – 0.54 whereas the highest data is 3.3 by Hwang et al. (2007).

Table 5.1.a Results for thermal-conductivity enhancement in SiO₂ – water nanofluids from this study

Author	Nominal SiO ₂ particle size (nm)	Volume fraction (%)	Thermal conductivity enhancement (%)	Reduced thermal conductivity enhancement and temperature	Measurement method
Present results	12	0.45	0.2	0.44 at 20°C	3 ω method
		1.85	1.0	0.54 at 20°C	
		4.0	2.2	0.55 at 20°C	

Table 5.1.b Comparison of thermal conductivity enhancement in SiO₂ – water nanofluids reported in the literature

Author	Nominal SiO ₂ particle size (nm)	Volume fraction (%)	Thermal conductivity enhancement (%)	Reduced thermal conductivity enhancement and temperature	Measurement method
Kang et al., (2006)	15 – 20	1.00	2.0	2.0	Transient hot wire
		2.00	2.6	1.3	
		3.00	3.8	1.3	
		4.00	5.0	1.3	
Hwang et al., (2006)	12	1.0	3.3	3.3	Transient hot wire
Wang et al., (2007)	23	1.0	2.8	2.8 at 20 °C	3 ω method

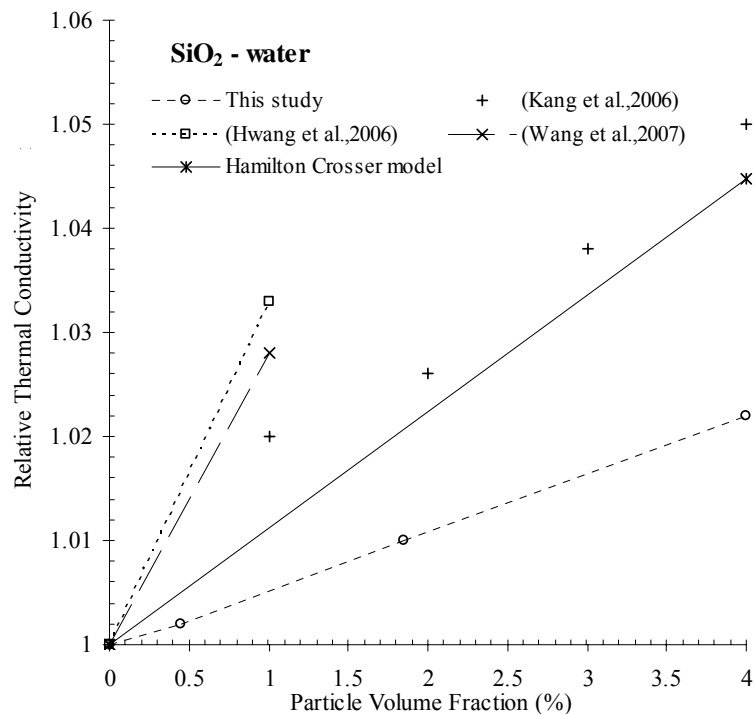


Figure 5.2 Comparison of our experimental results with selected results from literature for the relative thermal conductivity of SiO₂-water nanofluids

In Figure 5.2 we compared our experimental results with the other literature values, as well as classical effective thermal conductivity model, known as Hamilton – Crosser model(Hamilton & Crosser, 1962). Our experimental results for water based SiO₂ nanofluids are lower than the model and the other data from literature.

5.3.2.2 TiO₂ – water Nanofluids

The effective thermal conductivity of TiO₂-water nanofluids with concentrations of 0.2, 1.0, 2.0 and 3.0 volume % were measured at temperatures of 13 °C, 23 °C, 40 °C, and 55 °C. The comparison of our present results for the thermal conductivity enhancement of TiO₂-water nanofluids with the data of several groups from the literature is given in Table 5.2a and b.

Table 5.2.a Results for thermal-conductivity enhancement in TiO₂ – water nanofluids from this study

Author	Nominal TiO ₂ particle size (nm)	Volume fraction (%)	Thermal conductivity enhancement (%)	Reduced thermal conductivity enhancement and temperature	Measurement method
Present results	21	0.2	0.4	2.0 at 13 °C	3 ω method
		1.0	2.5	2.5 at 13 °C	
		2.0	4.2	2.1 at 13 °C	
		3.0	7.4	2.5 at 13 °C	
		0.2	0.3	1.5 at 23 °C	
		1.0	2.3	2.3 at 23 °C	
		2.0	4.3	2.2 at 23 °C	
		3.0	6.9	2.3 at 23 °C	
		0.2	0.5	2.5 at 40 °C	
		1.0	2.7	2.7 at 40 °C	
		2.0	4.8	2.4 at 40 °C	
		3.0	7.1	2.4 at 40 °C	
		0.2	0.3	1.5 at 55 °C	
		1.0	2.2	2.2 at 55 °C	
		2.0	4.5	2.3 at 55 °C	
3.0	7.2	2.4 at 55 °C			

Table 5.2.b Comparison of thermal conductivity enhancement in TiO₂ – water nanofluids reported in the literature

Author	Nominal TiO ₂ particle size (nm)	Volume fraction (%)	Thermal conductivity enhancement (%)	Reduced thermal conductivity enhancement and temperature	Measurement method
Masuda et al., (1993)	27	1.00	2.0	2.0 at 32 °C	Transient hot wire
		2.00	4.8	2.4 at 32 °C	
		3.25	8.0	2.5 at 32 °C	
		3.25	8.4	2.6 at 47 °C	
		3.10	7.5	2.4 at 87 °C	
		4.30	10.5	2.4 at 32 °C	
		4.30	10.8	2.5 at 47 °C	
		4.30	9.9	2.3 at 87 °C	
		0.5	1.5	3.0 at 18 °C	
		0.5	5.0	10.0 at 65 °C	
Wang et al., (2007)	26	1.0	3.1	3.1 at 18 °C	3 ω method
		1.0	6.0	6.0 at 43 °C	
		1.0	10.0	10.0 at 65 °C	
		2.0	4.6	2.3 at 18 °C	
		2.0	8.4	4.2 at 43 °C	
		2.0	13.3	6.7 at 65 °C	
		4.0	11.0	2.8 at 18 °C	
		4.0	15.0	3.8 at 43 °C	
		4.0	19.5	4.9 at 65 °C	
		0.6	1.4	2.3 at 10 °C	
Zhang et al., (2006)	40	1.2	3.1	2.6 at 10 °C	Transient short hot wire
		2.6	5.8	2.2 at 10 °C	
		1.2	3.6	3.0 at 30 °C	
		2.6	5.4	3.0 at 30 °C	
		0.6	1.1	2.1 at 40 °C	
		1.2	3.7	3.1 at 40 °C	
Yoo et al., (2007)	25	2.6	6.5	2.5 at 40 °C	Transient hot wire
		0.1	10.0	100	
		0.5	11.8	23.6	
		1.0	14.5	14.5	
He et al., (2007)	21	0.24	1.9	7.9 at 22 °C	Transient hot wire
		0.6	3.6	6.0 at 22 °C	
		1.18	7.5	6.4 at 22 °C	
		1.92	8.6	4.5 at 22 °C	
Pak, & Cho, (1998)	27	1.0	3.5	3.5	Transient hot wire
		2.0	5.0	2.5	
		3.0	7.7	2.6	
		4.0	12.0	3.0	
		0.5	4.5	9.0	
Murshed et al., (2005)	15	0.8	9.5	11.9	Transient hot wire
		1.0	18.5	18.5	
		2.0	23.5	11.8	
		3.0	25.5	8.5	
		4.0	27.5	6.9	
Wen, & Ding, (2006)	34	5.0	30.0	5.9	Transient hot wire
		0.29	1.8	6.2	
		0.41	3.1	7.6	
		0.53	5.1	9.6	
		0.68	6.3	9.3	

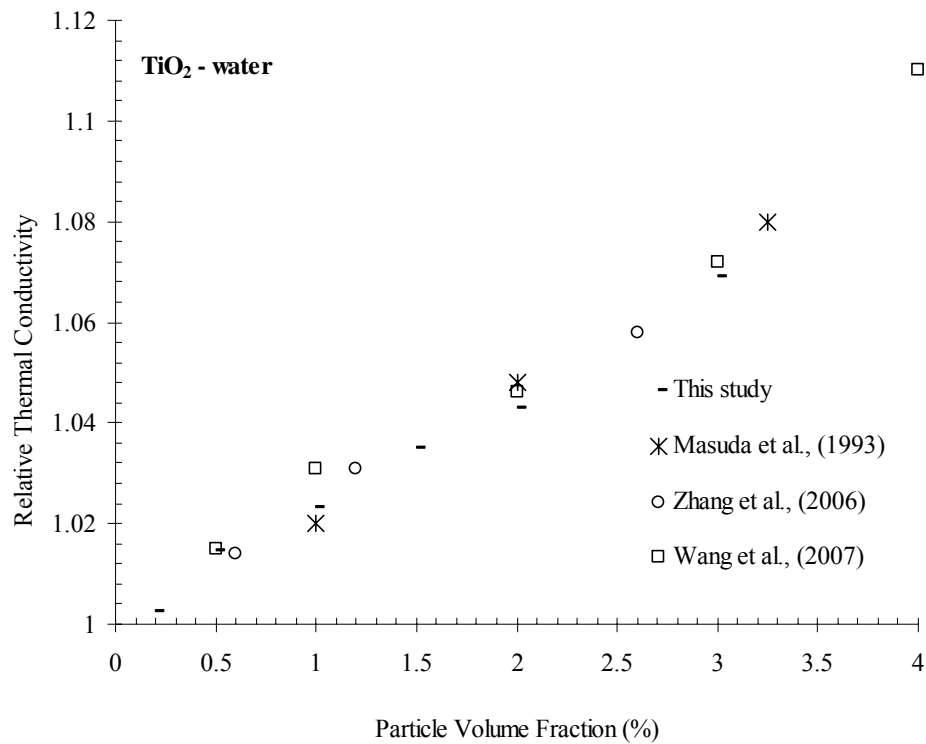


Figure 5.3 Experimental results of relative thermal conductivity of TiO₂ nanofluids, for room temperature (23 °C for our data), compared to selected literature data

In Figure 5.3 we have presented our experimental data for the relative thermal conductivity at room temperature (23 °C for our data), which shows good agreement with selected literature data (Masuda et al., 1993; Zhang et al., 2006; Wang et al., 2007). Whereas other data (Murshed et al., 2005; Wen & Ding, 2006; Yoo et al., 2007; He et al., 2007; Wang et al., 2007) show anomalous enhancement for the effective thermal conductivity of TiO₂–water nanofluids, which can not be explained with classical models such as Maxwell, Hamilton-Crosser or Bruggeman.

In Figure 5.4 we have compared our experimental data with the classical models Hamilton-Crosser and Bruggeman and as well as a new model (Xie et al. 2005). From the figure it can be seen that our data show reasonably good agreement with Hamilton – Crosser model.

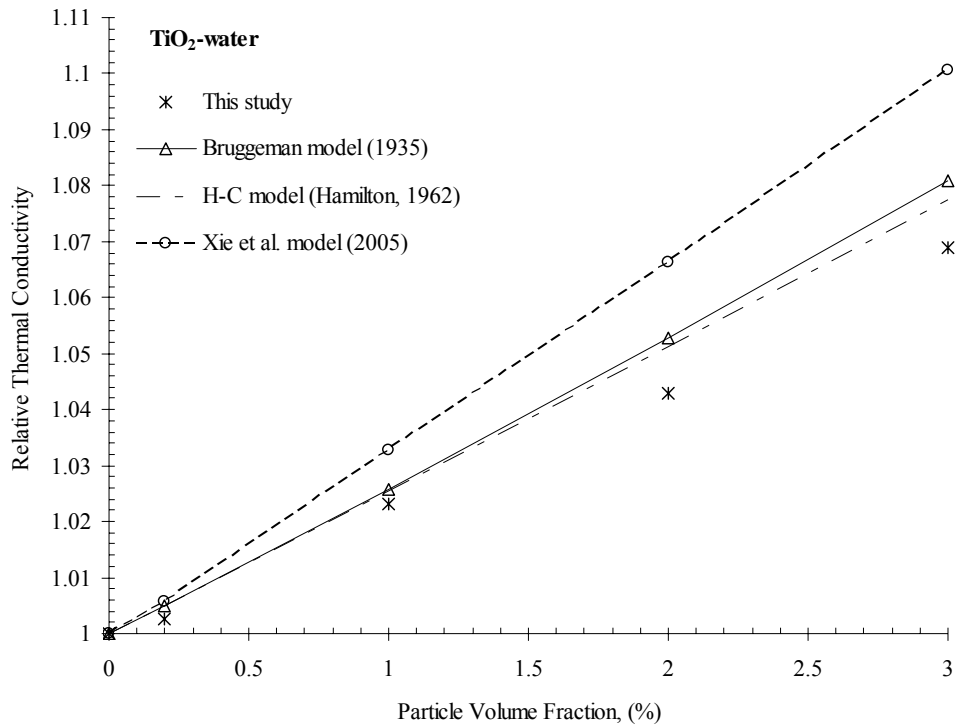


Figure 5.4 Experimental data for the relative thermal conductivity of TiO₂ nanofluids from this study, compared to models

As indicated in the introduction of this chapter in the literature there are several papers pointing out that the thermal conductivity ratio of nanofluid to base fluid (relative thermal conductivity) increases with increasing temperature. For the case of water-based nanofluids containing TiO₂ spherical nanoparticles, there are few reports on the temperature dependence (Masuda et al. 1993; Zhang et al. 2006; Wang et al. 2007). We compare our results with these data, for selected nanoparticle volumetric fractions between 2.0 % and 4.0 %, for the relative thermal conductivity in Figure 5.5.

As it is seen from Figure 5.5, our data show similar behavior with Masuda et al. (1993) and Zhang et al. (2006) in that the thermal conductivity of nanofluids is not much more temperature dependent than that of the base fluid. While on the contrary, Wang et al. (2007) concluded in their study that the relative thermal conductivity of TiO₂-water nanofluids is temperature dependent.

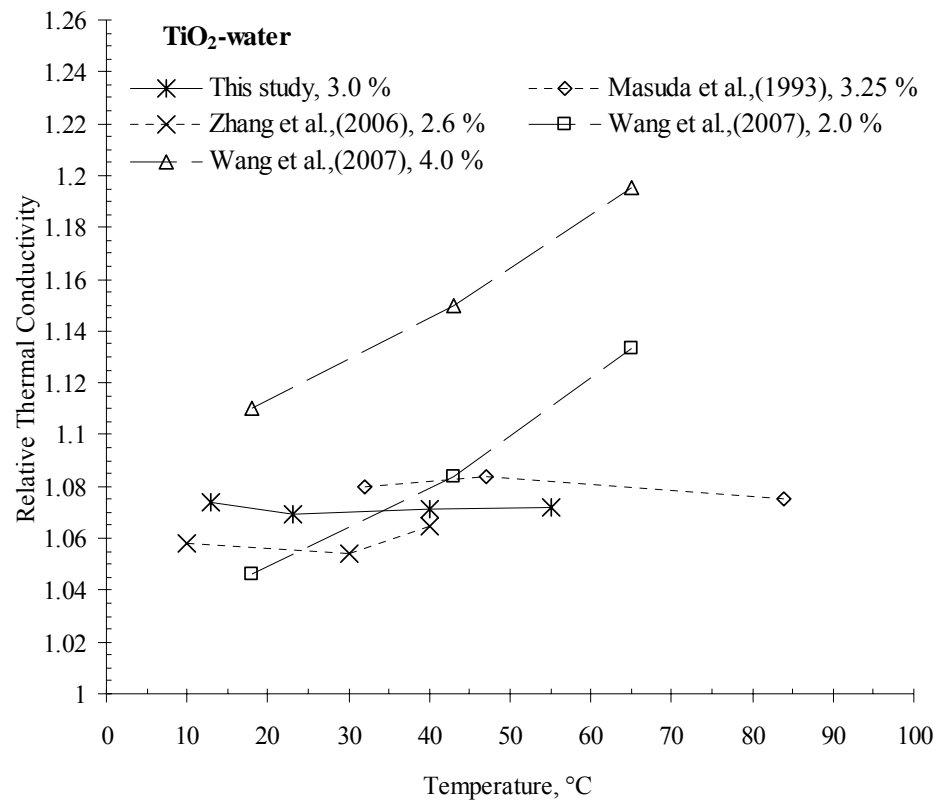


Figure 5.5 Temperature dependence of relative thermal conductivity of TiO₂-water nanofluids.

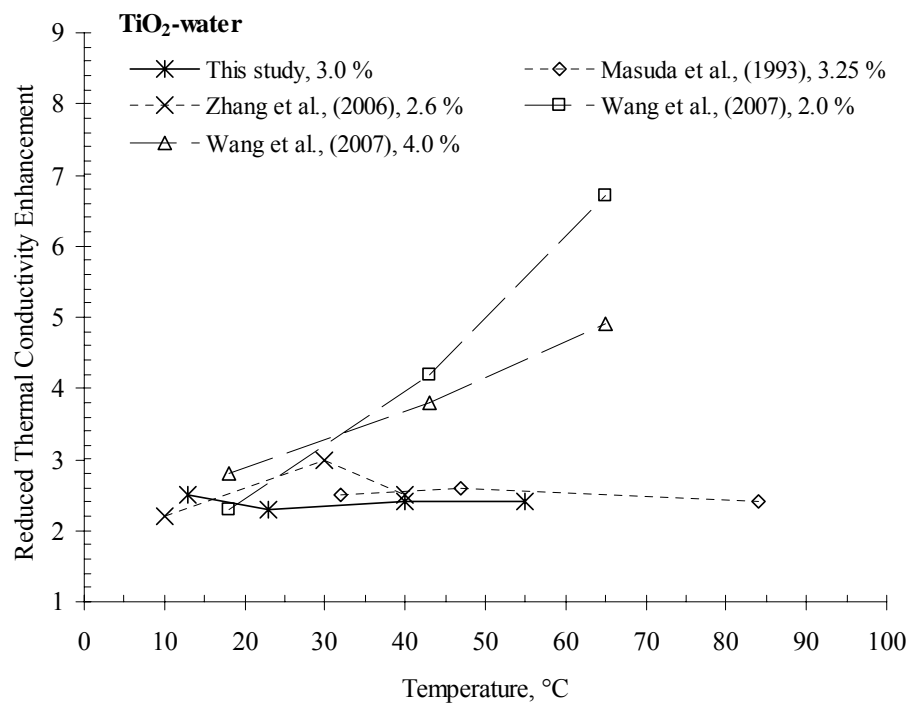


Figure 5.6 Comparisons of reduced thermal conductivity enhancement versus temperature of TiO₂-water nanofluids, results from the literature and this study

Figure 5.6 depicts that for the temperature range of 10 °C to 30 °C all reduced thermal conductivity enhancement values are in the range of 2 and 3. Eventhough our values and the values of Masuda et al. (1993) and Zhang et al. (2006) in the range of 2 and 3 for the temperatures over 30 °C, results of Wang et al. (2007) show an increase to 7 for 65°C.

5.3.2.3 Al_2O_3 – water Nanofluids

The effective thermal conductivity of Al_2O_3 -water nanofluids with concentrations of 0.5 to 5.0 volume % were measured at temperatures 20°C. Also the experiments were performed at 35 °C and 50 °C for the concentrations of 0.5 and 1.5 volume %. The comparison of our present results for the thermal conductivity enhancement of Al_2O_3 -water nanofluids with the data of several groups from the literature is given in Table 5.3a and b.

Table 5.3.a Results for thermal-conductivity enhancement in Al_2O_3 – water nanofluids from this study

Author	Nominal Al_2O_3 particle size (nm)	Volume fraction (%)	Thermal conductivity enhancement (%)	Reduced thermal conductivity enhancement and temperature	Measurement method
Present results	25	0.5	0.8	1.6 at 20 °C	3 ω method
		1.0	1.4	1.4 at 20 °C	
		1.5	2.3	1.5 at 20 °C	
		2.0	2.7	1.4 at 20 °C	
		3.0	3.9	1.3 at 20 °C	
		4.0	5.3	1.3 at 20 °C	
		5.0	6.5	1.3 at 20 °C	
		0.5	1.0	2.0 at 35 °C	
		1.5	2.5	1.7 at 35 °C	
		0.5	1.0	2.0 at 50 °C	
1.5	2.5	1.7 at 50 °C			

Table 5.3.b Comparison of thermal conductivity enhancement in Al_2O_3 – water nanofluids reported in the literature

Author	Nominal Al_2O_3 particle size (nm)	Volume fraction (%)	Thermal conductivity enhancement (%)	Reduced thermal conductivity enhancement and temperature	Measurement method
Masuda et al., (1993)	13	1.3	10.5	8.0 at 32 °C	Transient hot wire
		1.3	10.0	7.7 at 47 °C	
		1.3	9.0	6.9 at 67 °C	
		4.0	32.0	8.0 at 32 °C	
		4.0	31.0	7.8 at 47 °C	

Lee et al., (1999)	28	1.0	2.5	2.5	Transient hot wire
		2.0	5.0	2.5	
		3.0	7.5	2.5	
		4.0	9.0	2.3	
		4.3	10.0	2.3	
Wang et al., (1999)	28	3.0	11.0	3.7 at 24 °C	Steady state parallel plate
		4.5	14.0	3.1 at 24 °C	
		5.5	15.0	2.7 at 24 °C	
		1.0	2.2	2.2 at 21 °C	
		1.0	5.2	5.2 at 31 °C	
Das et al., (2003)	38	1.0	8.7	8.7 at 41 °C	Temperature oscillation
		1.0	10.5	10.5 at 51 °C	
		4.0	9.5	2.4 at 21 °C	
		4.0	13.0	3.2 at 31 °C	
		4.0	19.5	4.9 at 41 °C	
		4.0	24.5	6.1 at 51 °C	
		1.2	5.0	4.2 at 10 °C	
		2.6	7.5	2.9 at 10 °C	
		4.3	10.0	2.3 at 10 °C	
		6.0	12.0	2.0 at 10 °C	
Zhang et al., (2006)	20	1.2	5.0	4.2 at 30 °C	Transient short hot wire
		2.6	7.5	2.9 at 30 °C	
		4.3	10.0	2.3 at 30 °C	
		6.0	12.0	2.0 at 30 °C	
		1.2	5.0	4.2 at 50 °C	
		2.6	7.5	2.9 at 50 °C	
		4.3	10.0	2.3 at 50 °C	
		6.0	12.0	2.0 at 50 °C	
		0.5	3.0	6.0 at 28 °C	
		2.0	7.7	3.9 at 28 °C	
Li & Peterson, (2007)	36	4.0	9.3	2.3 at 28 °C	Steady state cut-bar
		6.0	11.0	1.8 at 28 °C	
		0.5	6.3	12.6 at 35 °C	
		2.0	18.1	9.1 at 35 °C	
		4.0	25.2	6.3 at 35 °C	
		6.0	28.0	4.7 at 35 °C	
Timofeeva et al.,(2007)	20	2.5	3.0	1.2 at 23 °C	Transient hot wire
		5.0	7.0	1.4 at 23 °C	
		1.0	3.5	3.6 at 20 °C	
Murshed et al., (2008)	80	1.0	6.2	6.2 at 30 °C	Transient hot wire
		1.0	8.7	8.7 at 40 °C	
		1.0	9.5	9.5 at 50 °C	
		1.0	12.0	12.0 at 60 °C	

In Figure 5.7 we have presented our experimental data for the relative thermal conductivity at room temperature (20 °C for our data), which exhibits good agreement with data of Timofeeva et al. (2007) whereas the other selected literature data (Lee et al., 1999; Wang et al., 1999; Das et al., 2003; Zhang et al., 2006; Li & Peterson, 2007) indicate higher enhancement for the effective thermal conductivity of Al₂O₃ - water nanofluids.

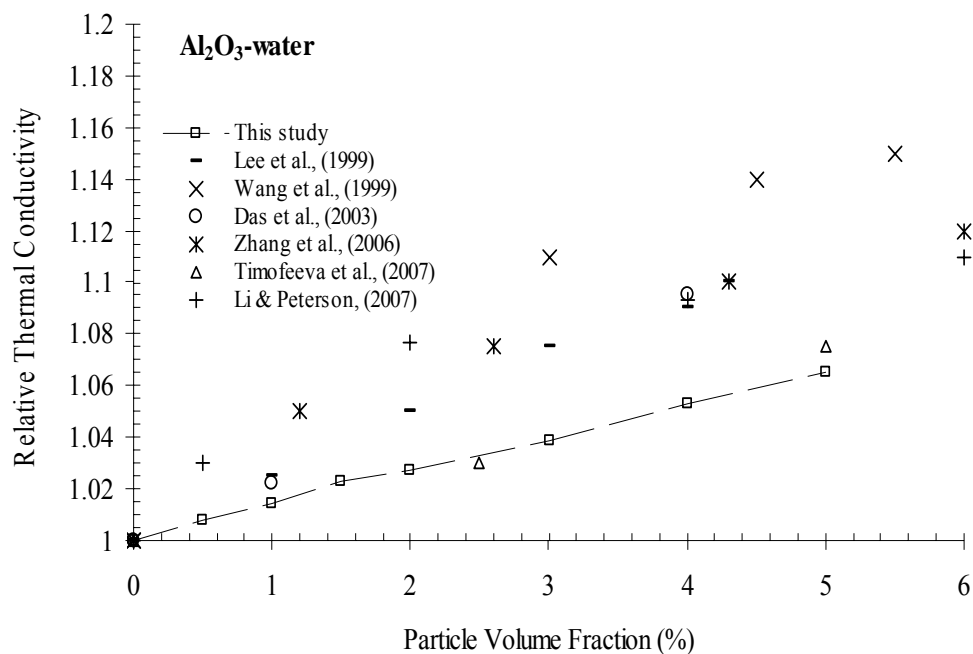


Figure 5.7 Experimental results of relative thermal conductivity of Al₂O₃ - water nanofluids, for room temperature (20 °C for our data), compared to selected literature data.

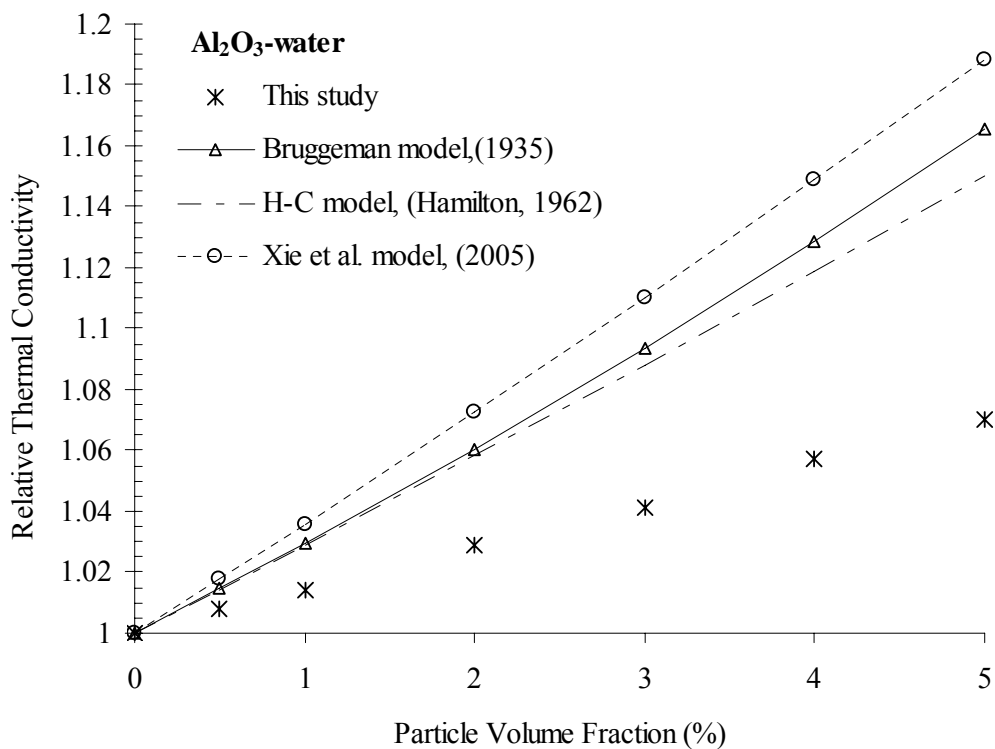


Figure 5.8 Experimental data for the relative thermal conductivity of Al₂O₃ - water nanofluids from this study, compared to models.

In Figure 5.8 we have compared our experimental data with Hamilton-Crosser (1962), Bruggeman (1935), and Xie et al. (2005) models. From the figure it can be seen that for 5 % volume concentration enhancement in thermal conductivity is 6.5 % whereas this increment is from 15 % to 19 % for the models discussed.

Effect of temperature on the enhancement of thermal conductivity of nanofluids is demonstrated in Figure 5.9 for Al_2O_3 – water nanofluids. Figure 5.9 compares our data for 1.5% volumetric concentration of nanoparticles and the data reported by Masuda et al. (1993) for 1.3 %, Das et al. (2003) for 1 %, Zhang et al. (2006) for 1.2 % and Murshed et al. (2008b) for 1 %, volumetric loading of nanoparticles. For the measurements at 20°C, our results are similar with Das et al. (2003) and Murshed et al., (2008). Nevertheless with the increase of temperature, relative thermal conductivity of our nanofluids is not increasing, which is in contradiction with the data of Das et al. (2003) and Murshed et al. (2008b). On the one hand the relative thermal conductivity result of Masuda et al. (1993) and Zhang et al. (2006) has similarity with our result which is not increasing with the temperature; on the other hand their results are considerably higher than ours.

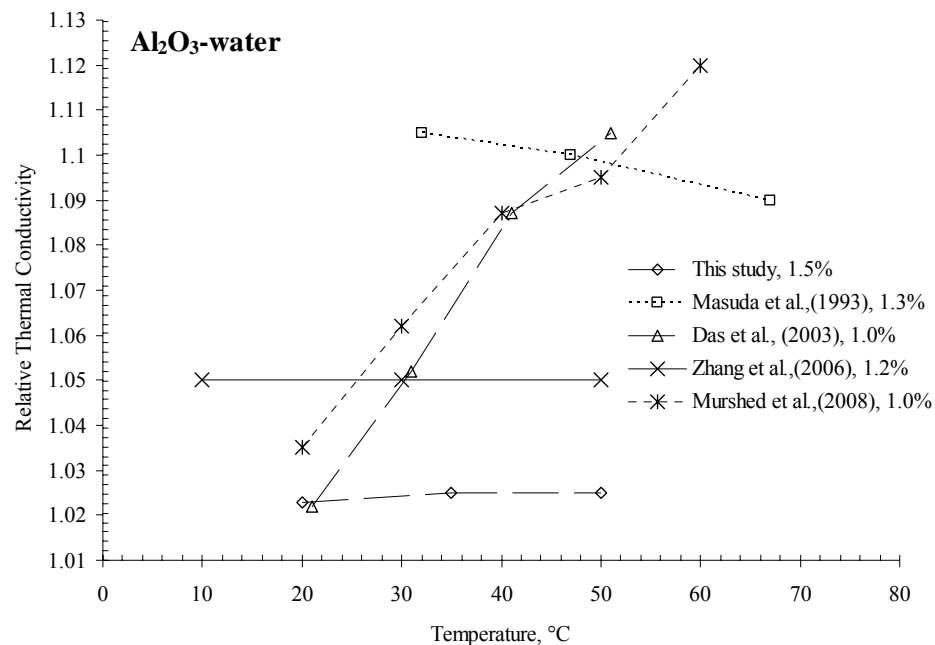


Figure 5.9 Effect of temperature on the relative thermal conductivity for Al_2O_3 -water nanofluids.

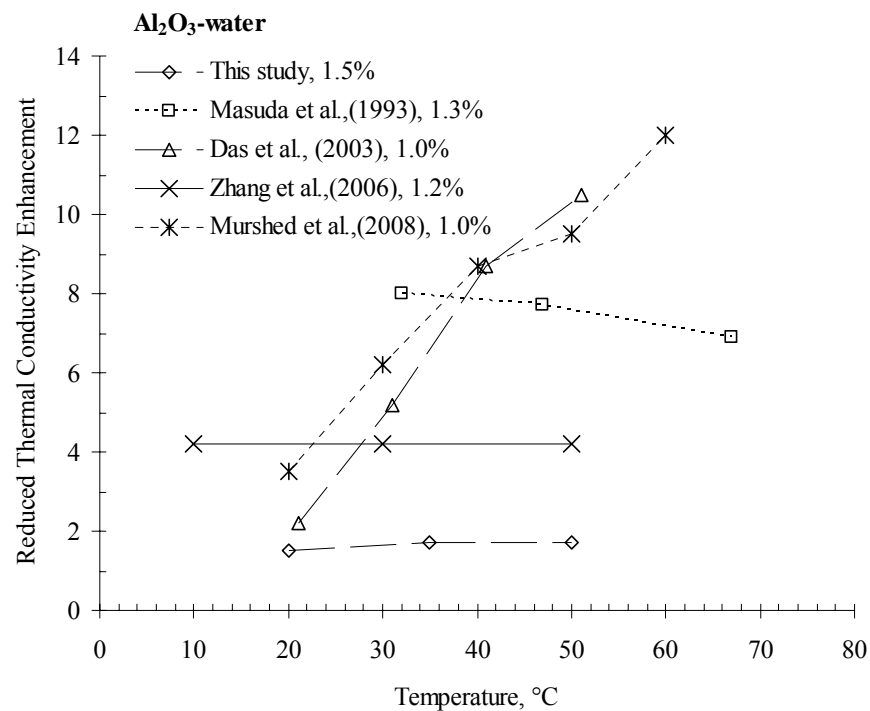


Figure 5.10 Comparisons of reduced thermal conductivity enhancement versus temperature of Al₂O₃ - water nanofluids, results from the literature and this study.

Figure 5.10 denotes that for the temperature range of 10 °C to 20 °C all reduced thermal conductivity enhancement values are in the range of 1.3 to 4 except for Masuda et al. (1993). In spite of the fact that our values and the values of Masuda et al. (1993) and Zhang et al. (2006) are not increasing with the temperature, results of Das et al. (2003) and Murshed et al. (2008b) increase from 2.2 to 10.5 and 3.6 to 12.0 respectively, in the range of temperature 20°C to 60°C.

5.3.2.4 Al₂O₃ –EG(Ethylene Glycol) Nanofluids

The effective thermal conductivity of Al₂O₃-EG nanofluids with concentrations of 0.5 to 5.0 volume % were measured at 20°C. The comparison of our present results for the thermal conductivity enhancement of Al₂O₃-water nanofluids with the data of several groups from the literature is given in Table 5.4a and b.

Table 5.4.a Results for thermal-conductivity enhancement in Al₂O₃ – EG nanofluids from this study

Author	Nominal Al ₂ O ₃ particle size (nm)	Volume fraction (%)	Thermal conductivity enhancement (%)	Reduced thermal conductivity enhancement and temperature	Measurement method
Present results	25	0.5	2.0	4.0 at 20 °C	3 ω method
		1.0	3.2	3.2 at 20 °C	
		2.0	6.0	3.0 at 20 °C	
		3.0	8.4	2.8 at 20 °C	
		4.0	11.0	2.8 at 20 °C	
		5.0	13.3	2.7 at 20 °C	

Table 5.4.b Comparison of thermal conductivity enhancement in Al₂O₃ – EG nanofluids reported in the literature

Author	Nominal Al ₂ O ₃ particle size (nm)	Volume fraction (%)	Thermal conductivity enhancement (%)	Reduced thermal conductivity enhancement and temperature	Measurement method
Lee et al., (1999)	28	1.0	2.5	2.5	Transient hot wire
		2.0	6.0	3.0	
		3.0	10.0	3.3	
		4.0	13.0	3.3	
		5.0	18.0	3.6	
Timofeeva et al.,(2007)	20	1.0	2.0	2.0 at 23 °C	Transient hot wire
		2.5	5.5	2.2 at 23 °C	
		5.0	13.0	2.6 at 23 °C	
Oh et al., (2008)	45	1.0	1.9	1.9 at 21 °C	3 ω method
		2.0	2.7	1.4 at 21 °C	
		3.0	7.5	2.5 at 21 °C	
		4.0	9.7	2.4 at 21 °C	

In Figure 5.11 we have presented our experimental data for the relative thermal conductivity at room temperature (20 °C for our data), which shows good agreement with data of Timofeeva et al. (2007) and Oh et al. (2008). Also for the low volume fraction, result of Lee et al. (1999) is consistent with ours, whereas for the volume concentration over 3 %, they found higher relative thermal conductivity values. For the 5 % volume fraction we have found 13.3 % increase, Lee et al. (1999) reported an enhancement 18 % for the same volume fraction.

In Figure 5.12 we have compared our experimental data with Hamilton-Crosser (1962), Bruggeman (1935), and Xie et al. (2005) models. From the figure it can be seen that contrary to water-based nanofluids, ethylene glycol based Al₂O₃ nanofluid is consistent with Hamilton-Crosser model.

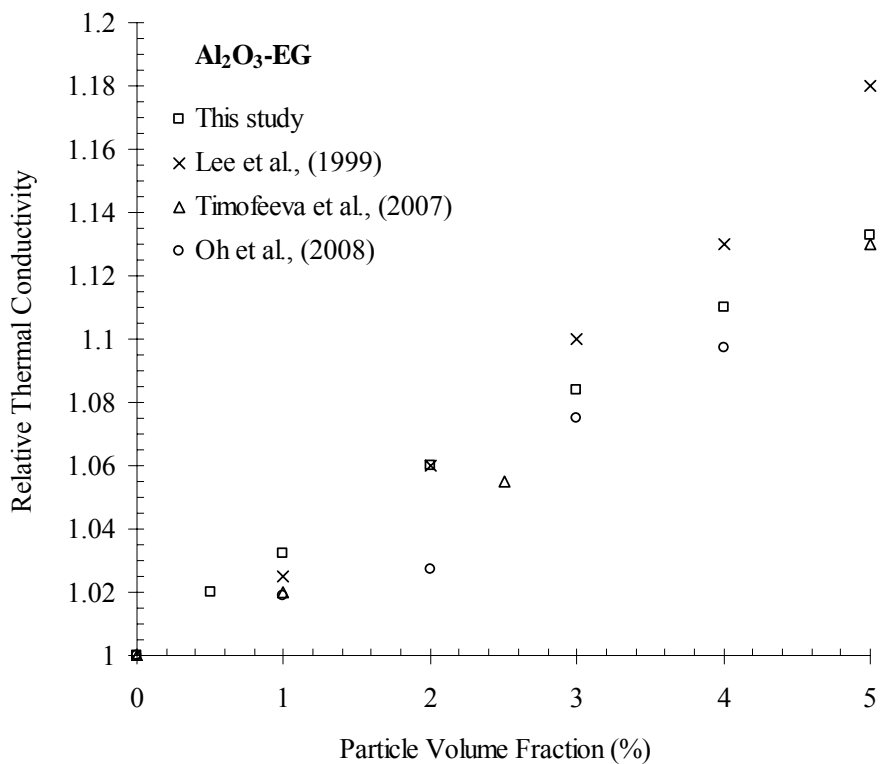


Figure 5.11 Experimental results of relative thermal conductivity of Al₂O₃ – EG nanofluids, for room temperature (20 °C for our data), compared to selected literature data.

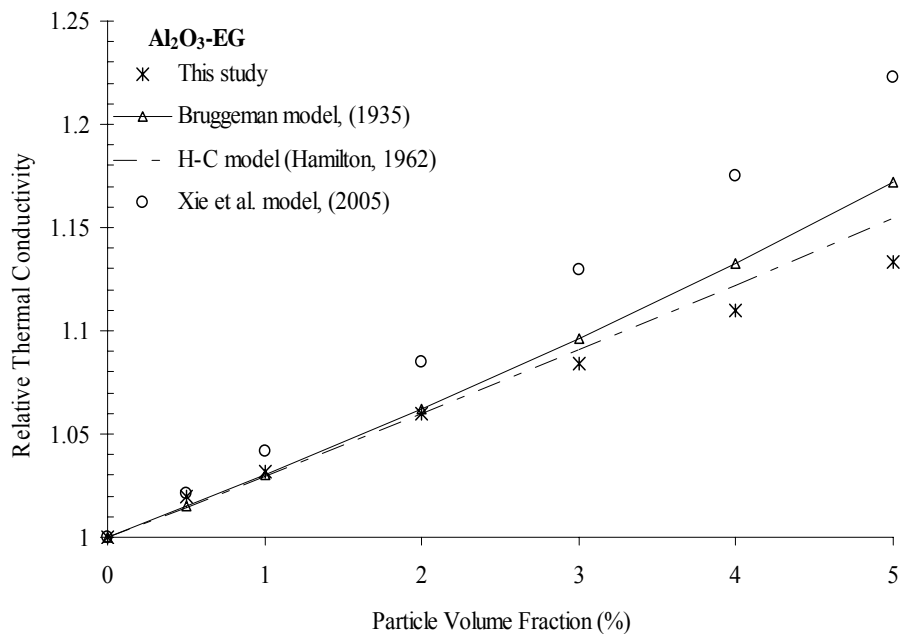


Figure 5.12 Experimental data for the relative thermal conductivity of Al₂O₃ - EG nanofluids from this study, compared to models.

5.3.3 Effect of Particle Conductivity

In Figure 5.13 we compared our experimental results for water based SiO_2 , Al_2O_3 and TiO_2 nanofluids. Inasmuch as the thermal conductivity of SiO_2 is very low compared with the other samples, it has the lower enhancement. Moreover, comparison of the TiO_2 nanofluids with the Al_2O_3 nanofluids showed that the highly thermal conductive material is not always the excellent application for enhancing the thermal transport property of nanofluids. Thermal conductivity of TiO_2 – water nanofluid possesses higher enhancement than the Al_2O_3 – water nanofluid, even TiO_2 bulk thermal conductivity value is lower than the Al_2O_3 . Similar result was presented by (Hong, Hong & Yang, 2006) for Fe nanofluids compared with the Cu nanofluids.

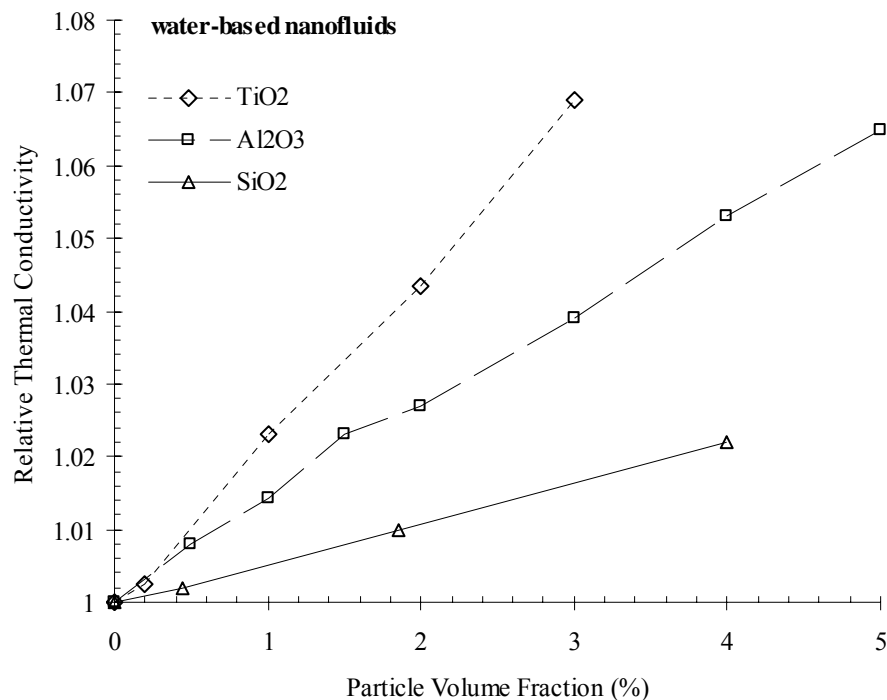


Figure 5.13 Relative thermal conductivity versus particle volume fraction of TiO_2 , Al_2O_3 and SiO_2 nanofluids.

5.3.4 Effect of Surfactant

It is suggested that by the use of surfactant more stable nanofluids can be achieved (Trisaksri & Wongwises, 2007). Although surfactants have been used by some groups during production process of nanofluids, there are few systematic studies (Li

X.F. et al., 2008; Zhu et al., 2009) on effect of surfactant on thermal conductivity of nanofluids. For observing this effect we have used sodium dodecylbenzenesulfonate (SDBS) as a surfactant and mixed it to pure de-ionized water at different mass ratio of SDBS/ Al_2O_3 . It was observed that the thermal conductivity of SDBS – water mixture decreased with the increasing SDBS ratios which means that the effect of this surfactant was to decrease the thermal conductivity of the base fluid (Figure 5.14). We further used this surfactant in 1 % by volume Al_2O_3 – water nanofluids at different ratio of SDBS/ Al_2O_3 , as it can be seen from Figure 5.14, its effect on thermal conductivity was still negative. In other words, thermal conductivity of Al_2O_3 – water nanofluids was better than with the same nanofluid with surfactant. In our case surfactant did not have positive effect on effective thermal conductivity of nanofluids.

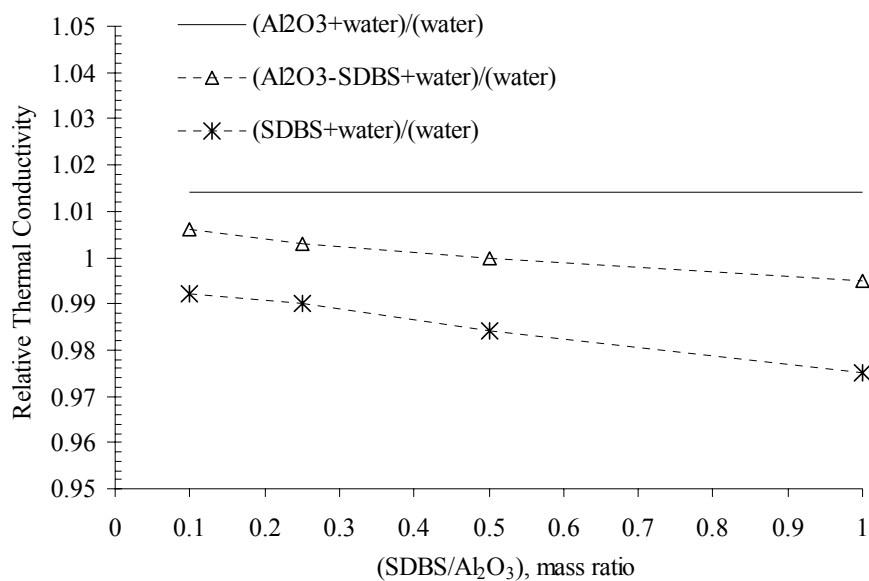


Figure 5.14 Effect of SDBS surfactant on relative thermal conductivity of 1 % by volume Al_2O_3 – water nanofluids at different mass ratio of SDBS/ Al_2O_3 .

5.3.5 Effect of Base-fluid

The effect of base-fluid on relative thermal conductivity of nanofluids is depicted in Figure 5.15 for two base-fluids, water and ethylene glycol. The results show higher relative thermal conductivity for poorer (lower thermal conductivity) heat

transfer fluid (ethylene glycol). Even though this tendency was not supported in all experimental studies (Oh et al., 2009) reviewed, it was commonly the case (Wang et al., 1999; Lee et al., 1999; Timofeeva et al., 2007) .

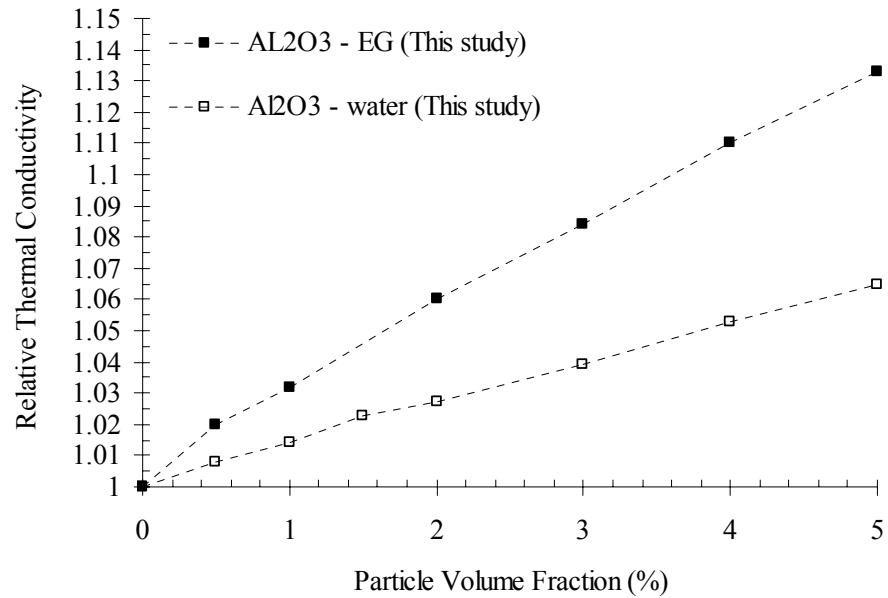


Figure 5.15 Effect of base-fluid material for Al₂O₃ in water and EG.

5.4 Conclusion

Thermal conductivities of SiO₂-water, TiO₂-water, Al₂O₃-water and Al₂O₃-EG nanofluids were measured using a 3 ω method for different particle concentrations and temperatures.

For SiO₂-water nanofluids, thermal conductivity measurements were done at 20 °C with volume fractions 0.45, 1.85 and 4.0 %, and the enhancement of the thermal conductivities were found 0.2, 1.0 and 2.2 %, respectively.

Measurements of thermal conductivity of TiO₂-water nanofluids for volume fractions ranging from 0.2 % to 3.0 % were made at varying temperatures from 13°C to 55°C showed that there is no dependence related to temperature; the thermal

conductivity increased by the same order of magnitude as the base fluid which is water. Also our measurements with Al_2O_3 -water were given the similar results with TiO_2 -water nanofluids on temperature dependency.

Moreover, comparison of the TiO_2 nanofluids with the Al_2O_3 nanofluids showed that the highly thermal conductive material is not always the excellent application for enhancing the thermal transport property of nanofluids. Thermal conductivity of TiO_2 – water nanofluid has higher enhancement than the Al_2O_3 – water nanofluid, even TiO_2 bulk thermal conductivity value is lower than the Al_2O_3 .

For observing the effect of surfactant on thermal conductivity of nanofluids we have used sodium dodecylbenzenesulfonate (SDBS). We used this surfactant in 1 % by volume Al_2O_3 – water nanofluids at different ratio of SDBS/ Al_2O_3 , and found that in our case surfactant did not have positive effect on effective thermal conductivity of nanofluids.

The effect of base-fluid on relative thermal conductivity of nanofluids was investigated with two base-fluids, water and ethylene glycol. Al_2O_3 nanoparticles for volume fractions in the range of 0.5 % to 5.0 % were compared at 20°C. The results show higher relative thermal conductivity for poorer (lower thermal conductivity) heat transfer fluid (ethylene glycol).

The experimental results expressed that the thermal conductivity enhancements were relatively in good agreement with the Hamilton-Crosser model, and they were moderated increases, not as high and sometimes qualified as anomalous increases as claimed by some researchers.

CHAPTER SIX

VISCOSITY OF NANOFUIDS

6.1 Introduction

Now that viscosity is a fundamental characteristic property of a fluid that influences flow and heat transfer phenomena, determining the viscosity of nanofluids is necessary for optimizing pumping costs of heat transfer applications. There are some studies on the viscosity of nanofluids (Masuda et al., 1993; Pak & Cho, 1998; Wang X. et al., 1999; Prasher, Song & Wang, 2006; Kang et al., 2006; Wang T. et al., 2007; Namburu, Kulkarni, Misra & Das, 2007; Nguyen et al., 2007; Timofeeva et al., 2007; Lee et al., 2008; Murshed et. al., 2008b; Anoop et al., 2009), but compared with the experimental studies on thermal conductivity, they are limited. Most of these reports show that the viscosity of nanofluids increased anomalously with increasing particle concentration, and it is not possible to predict this by classical models such as those of Einstein (1956), Krieger & Dougherty (1959) or Nielsen (1970).

Einstein (1956) proposed a viscosity correlation for a non-interacting particle suspension in a base fluid when the volume concentration is less than 5 %.

$$\mu_{\text{eff}} = \mu_1(1 + 2.5\phi) \quad (6.1)$$

where ϕ is the volume fraction of particles.

Krieger & Dougherty (1959) formulated a semi-empirical equation for relative viscosity expressed as

$$\mu_{\text{eff}} = \mu_1 \left(\frac{\phi}{\phi_m} \right)^{-[\eta]\phi_m} \quad (6.2)$$

where ϕ_m is the maximum packing fraction and $[\eta]$ is the intrinsic viscosity ($[\eta] = 2.5$ for hard spheres). For randomly mono-dispersed spheres, the maximum close packing fraction is approximately 0.64.

Another model was proposed by Nielsen (1970) for low concentration of particles. Nielsen's equation is as follows:

$$\mu_{\text{eff}} = \mu_1 (1 + 1.5\phi) e^{\phi / (1 - \phi_m)} \quad (6.3)$$

where ϕ and ϕ_m are the volume fraction of particles and the maximum packing fraction, respectively.

According to these models the effective viscosity depends on the viscosity of the base-fluid and on the volume fraction of particles. Nonetheless experimental studies show that the particle diameter, type of nanoparticle and the temperature may also affect the effective viscosity of nanofluids. To draw a clear conclusion for nanofluids, more experimental research is needed also for the effective viscosity of nanofluids.

In this chapter we present experimental measurements of the effective viscosity of nanofluids by using Sine-wave Vibro Viscometer, at different temperatures. We compare our experimental results with those in the literature also with some of the existing models.

6.2 Materials

We have prepared several nanofluids with varying particle volumetric concentrations such as SiO₂ – water (0.45, 1.85, 4.0% vol.), TiO₂ – water (0.2 to 3.0% vol.), Al₂O₃ – water (0.5 to 5.0% vol.) and Al₂O₃ – EG (0.5 to 5.0% vol.). In chapter 4 we have given the properties of the materials and preparation process of the nanofluids.

6.3 Experimental Setup and Procedure

The experimental setup for measuring the effective viscosity of nanofluids, consists of a Sine-wave Vibro Viscometer SV-10 and Haake temperature-controlled bath with a stability of 0.1 °C (Figure 6.1).

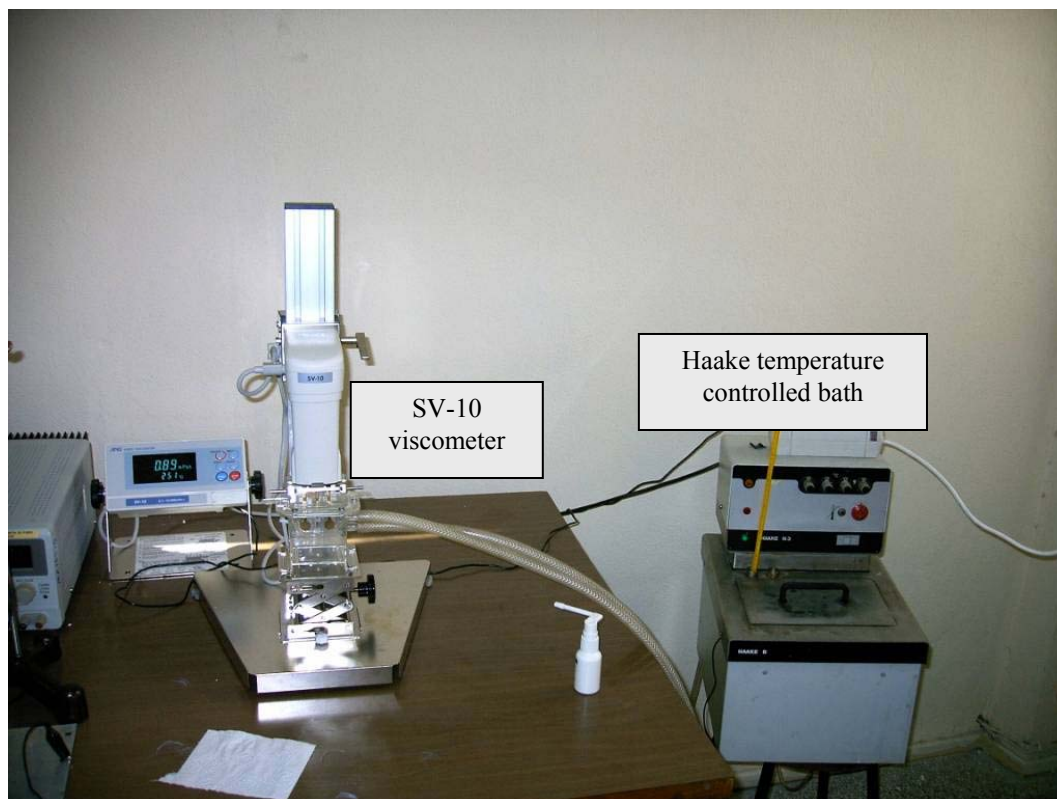


Figure 6.1 Sine-wave Vibro Viscometer SV-10 and Haake temperature-controlled bath.

The SV-10 viscometer manufactured by A&D Company Ltd.(Japan). This type is also known as “Sine Wave Vibro Viscometer”(Izumo & Koiwai, 2009) and the principle is different from conventional viscometers. It has two thin sensor plates that are driven with electromagnetic force at the same frequency by a sine-wave vibration in reverse phase like a tuning-fork. The electromagnetic drive controls the vibration of the sensor plates to maintain constant amplitude. The drive electric current, which is an exciting force, will be detected as the magnitude of the viscosity produced between the sensor plates and the sample fluid(Figure 6.2, (Izumo & Koiwai, 2009)).

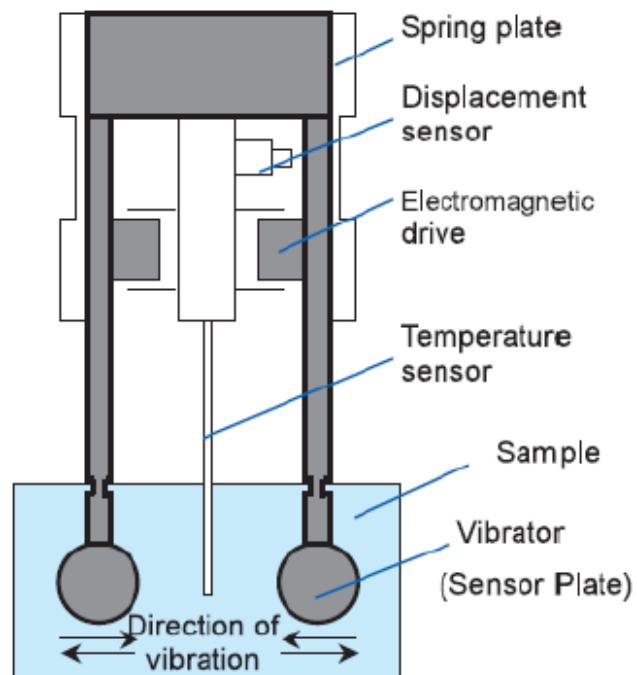


Figure 6.2 Schematic diagram of the vibro-viscometer



Figure 6.3 Vibrator (sensor plates) and water jacket

The coefficient of viscosity is obtained by the correlation between the drive electric current and the magnitude of the viscosity. Inasmuch as the viscosity is

dependent upon the temperature of the fluid, it is very important to measure the temperature of the fluid accurately. Using this viscometer we can determine an accurate temperature in a short period of time since the fluid and the detection unit (sensor plates) with small surface area, thermal capacity reaches thermal equilibrium in only a few seconds. The measurement range of viscosity is 0.3 mPa.s to 10,000 mPa.s. SV-10 vibrates with sine wave of frequency 30 Hz and amplitude approximately 0.2 mm (0.4 mm peak to peak).

To verify the accuracy of our system, the viscosity of base-fluids (water and ethylene glycol) was measured before and after from each experiment. The obtained results were compared with the data from literature (Lide, 2003).

6.4 Results and Discussion

6.4.1 Effect of Volume Fraction and Temperature

6.4.1.1 SiO₂ – water Nanofluids

Results of the viscosity measurements of SiO₂ – water nanofluids with concentration 0.45, 1.85 and 4.0 vol.% were measured at temperatures from 20°C to 50°C are given in Table 6.1. We present these results in Figure 6.4. On the one hand the viscosity of nanofluids increases dramatically, with an increase in particle concentration, on the other hand viscosity of these nanofluids show a similar decreasing behavior as water with the increase in temperature.

Table 6.1 Our experimental results for effective viscosity of SiO₂ – water nanofluids (mPa.s)

Samples	Temperature (°C)						
	20	25	30	35	40	45	50
water	1.00	0.89	0.8	0.72	0.65	0.6	0.55
SiO ₂ (0.45%)	1.10	1.00	0.88	0.81	0.76	0.65	0.60
SiO ₂ (1.85%)	1.88	1.68	1.55	1.41	1.25	1.13	1.05
SiO ₂ (4.0 %)	4.60	4.20	3.85	3.55	3.28	2.95	2.77

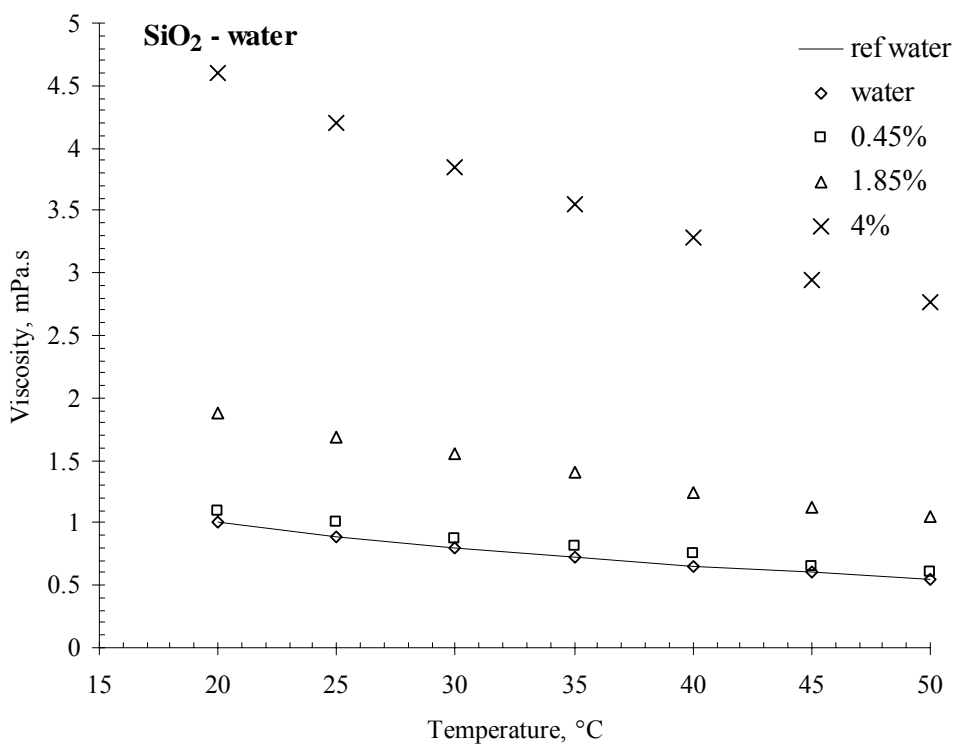


Figure 6.4 Effective viscosities of SiO₂-water nanofluids as a function of temperature

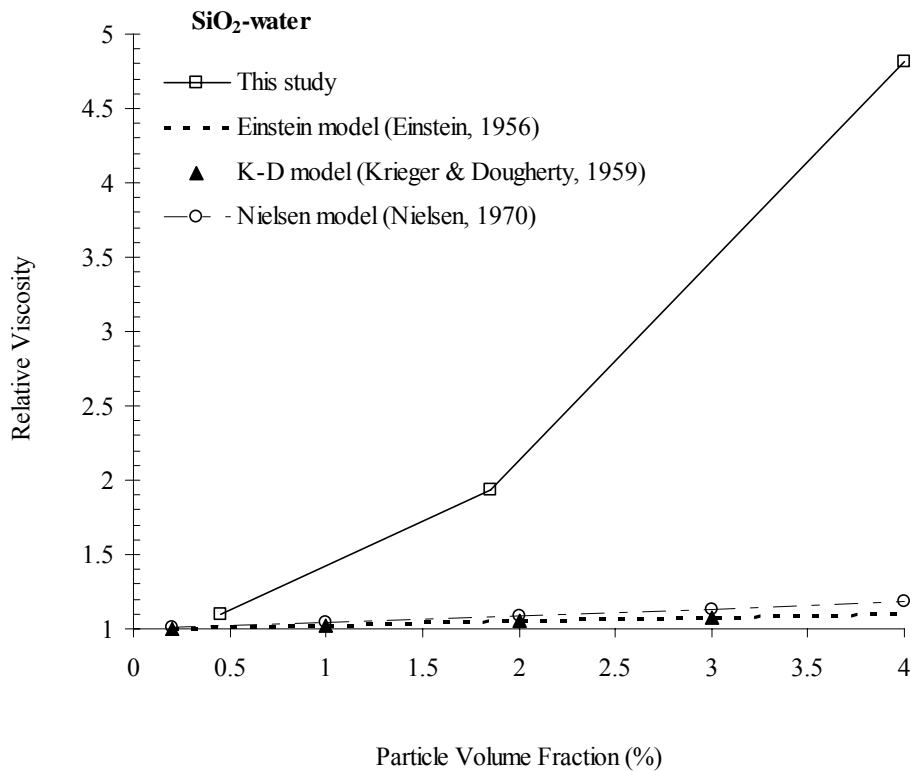


Figure 6.5 Relative viscosity of SiO₂-water nanofluids as a function of nanoparticle volume fraction at 20 °C

For SiO₂-water nanofluids, the experimental results are compared with the Einstein, Krieger & Dougherty and Nielsen models in Figure 6.5. It may be seen that measured viscosity values are well above the prediction of the models, the difference becoming larger as the volume concentration is increasing.

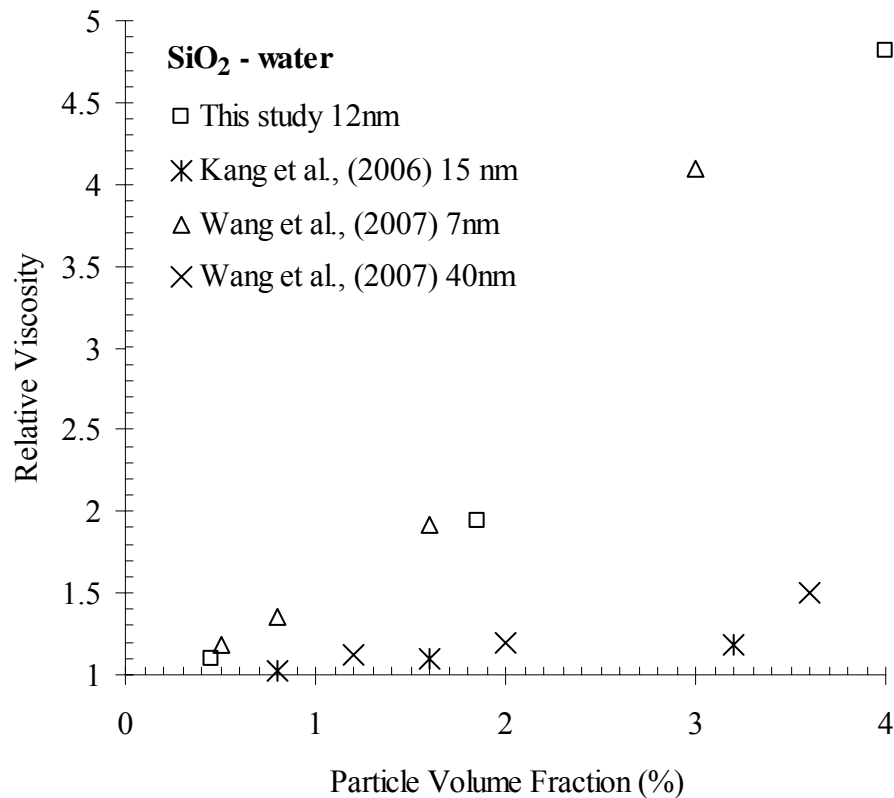


Figure 6.6 Experimental results of relative viscosity of SiO₂ nanofluids, for room temperature, compared to selected literature data

In Figure 6.6 our experimental results are compared with the existing literature values for the same nanofluids by Wang et al. (2007) for 7 nm and 40 nm particle sizes and Kang et al. (2006). Our experimental results are of the same as those by Wang et al. (2007) for the particle size of 7 nm, but larger than the other results.

6.4.1.2 TiO₂ – water Nanofluids

The effective viscosity values of TiO₂-water nanofluids with concentrations of 0.2, 1.0, 2.0 and 3.0 volume % were measured at temperatures from 13 °C to 55 °C

and given in Table 6.2 and plotted in Figure 6.7. As it is seen from the figure the results indicates similar behavior to SiO₂ nanofluids for volume fraction and temperature dependency.

Table 6.2 Our experimental results for effective viscosity of TiO₂ – water nanofluids (mPa.s)

Samples	Temperature (°C)							
	13	21	27.3	33.7	37.5	42.7	48.2	55
water	1.21	0.98	0.85	0.74	0.69	0.63	0.57	0.51
TiO ₂ (0.2%)	1.26	1.02	0.89	0.78	0.72	0.66	0.61	0.54
TiO ₂ (1.0%)	1.47	1.18	1.05	0.93	0.87	0.80	0.73	0.65
TiO ₂ (2.0%)	1.92	1.59	1.35	1.17	1.09	0.97	0.89	0.81
TiO ₂ (3.0%)	2.85	2.33	1.97	1.65	1.55	1.40	1.25	1.15

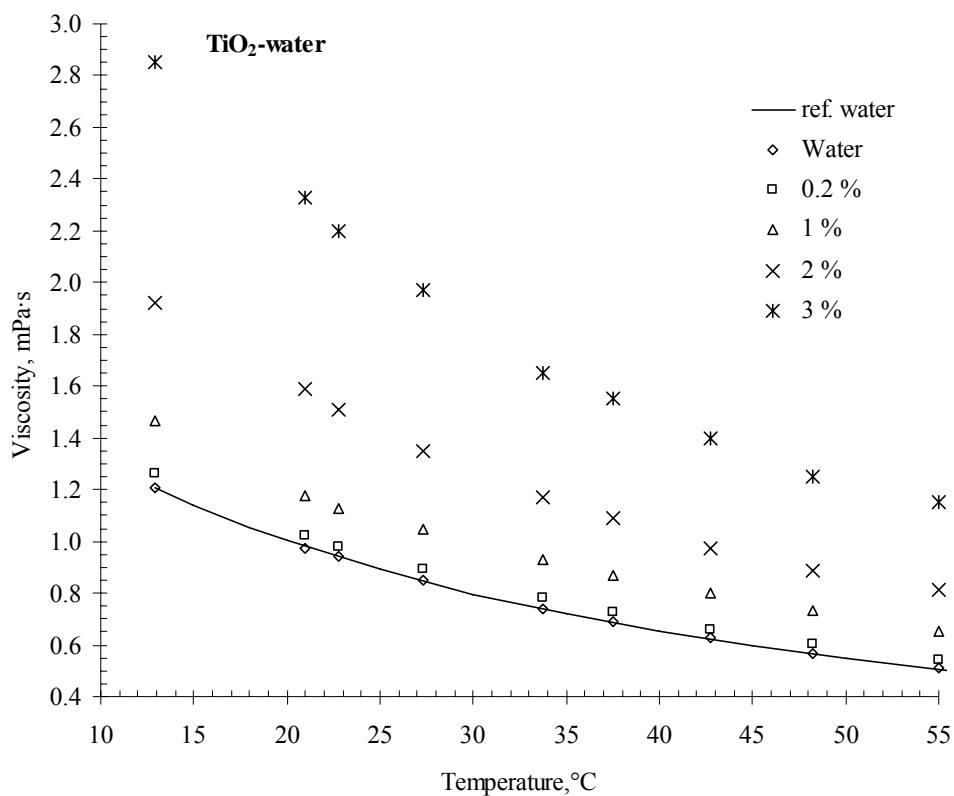


Figure 6.7 Effective viscosities of TiO₂–water nanofluids from 0.2 vol% to 3 vol% as a function of temperature

In Figure 6.8 and 6.9, we compared our experimental results on TiO₂-water nanofluids with the above cited models and the results of literature (Masuda et al., 1993, He et al., 2007 and Murshed et al., 2008b), respectively. Similar with our SiO₂ results model predictions are very low compared with experimental data.

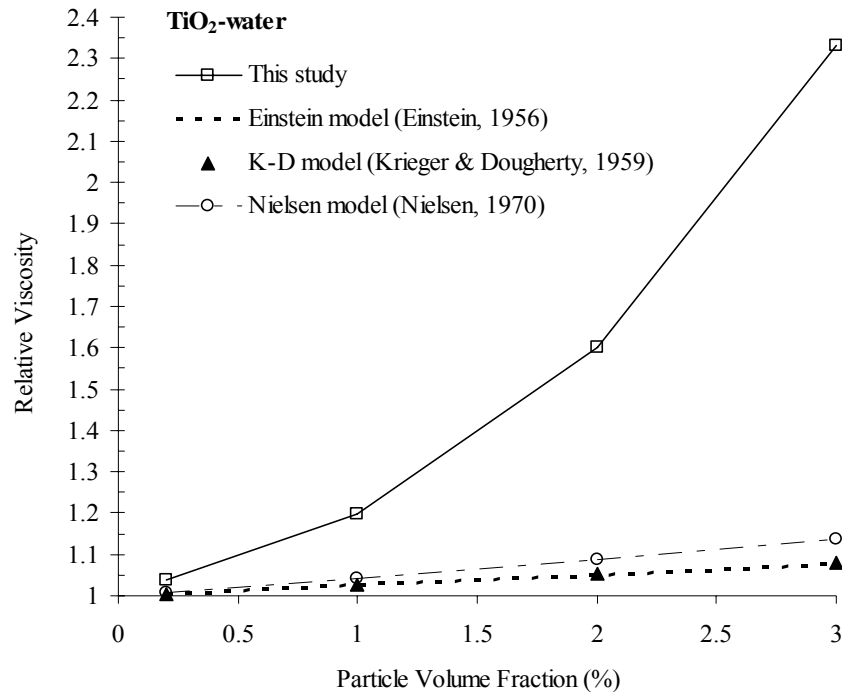


Fig. 6.8 Relative viscosity of TiO₂-water nanofluids as a function of nanoparticle volume fraction at 13 °C

As it is plotted in Figure 6.9, although relative viscosity values close to each other up to 1% volume fraction, with the increasing volume fraction our data is higher than the others. For 2% volume concentration Masuda et al. (1993) reported an increase in viscosity nearly 25%, where as our result with Murshed et al. (2008b) show an enhancement almost 65% at the same concentration. We have found an increase 135% for the maximum concentration 3%, but the enhancement reported by Murshed et al. (2008b) at the same concentration is only 75%.

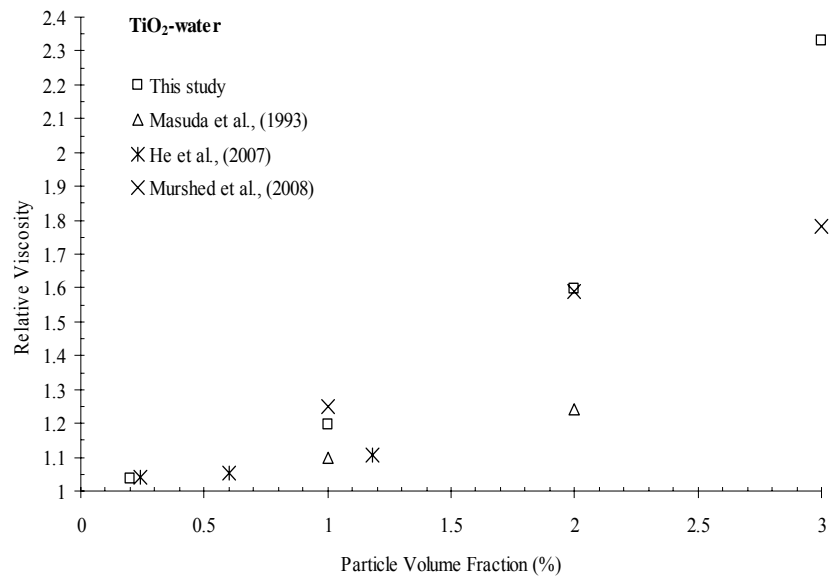


Figure 6.9 Experimental results of relative viscosity of TiO₂ nanofluids for room temperature compared to selected literature data

6.4.1.3 Al₂O₃ – water Nanofluids

The effective viscosity of Al₂O₃-water nanofluids with concentrations of 0.5 to 5.0 volume % were measured at temperatures from 20 °C to 50 °C and results are given in Table 6.3.

Table 6.3 Our experimental results for effective viscosity of Al₂O₃ – water nanofluids (mPa.s)

Samples	Temperature (°C)						
	20	25	30	35	40	45	50
water	1.00	0.89	0.8	0.72	0.65	0.6	0.55
Al₂O₃ (0.5%)	1.14	1.02	0.93	0.86	0.78	0.72	0.66
Al₂O₃ (1.0%)	1.44	1.17	1.08	0.99	0.93	0.87	0.83
Al₂O₃ (1.5%)	1.76	1.56	1.45	1.27	1.16	1.02	0.90
Al₂O₃ (2.0%)	2.25	1.91	1.70	1.55	1.41	1.25	1.15
Al₂O₃ (3.0%)	3.50	3.25	3.00	2.70	2.40	2.18	1.93
Al₂O₃ (4.0%)	5.18	4.68	4.28	3.90	3.53	3.27	3.06
Al₂O₃ (5.0%)	9.42	8.27	7.38	6.67	6.08	5.58	5.18

Our experimental viscosity values are also denoted in Figure 6.10 depending on temperature and particle volume fraction. Results point out similar tendency as the results of SiO₂-water and TiO₂-water nanofluids. While the viscosity of nanofluids increases dramatically, with an increase in particle concentration, the viscosity of these nanofluids show a similar decreasing behavior as water with the increase in temperature. We have observed almost 8 fold increase in viscosity for 5% volume fraction. This increment is the highest one among our water-based nanofluids. Maximum enhancement was 135 % for the maximum concentration 3% of TiO₂-water nanofluid, whereas this enhancement is 250 % for Al₂O₃-water nanofluid. At 4% volume fraction SiO₂-water nanofluid gave an increment 360 % whereas this increase is 418 % for Al₂O₃-water nanofluid.

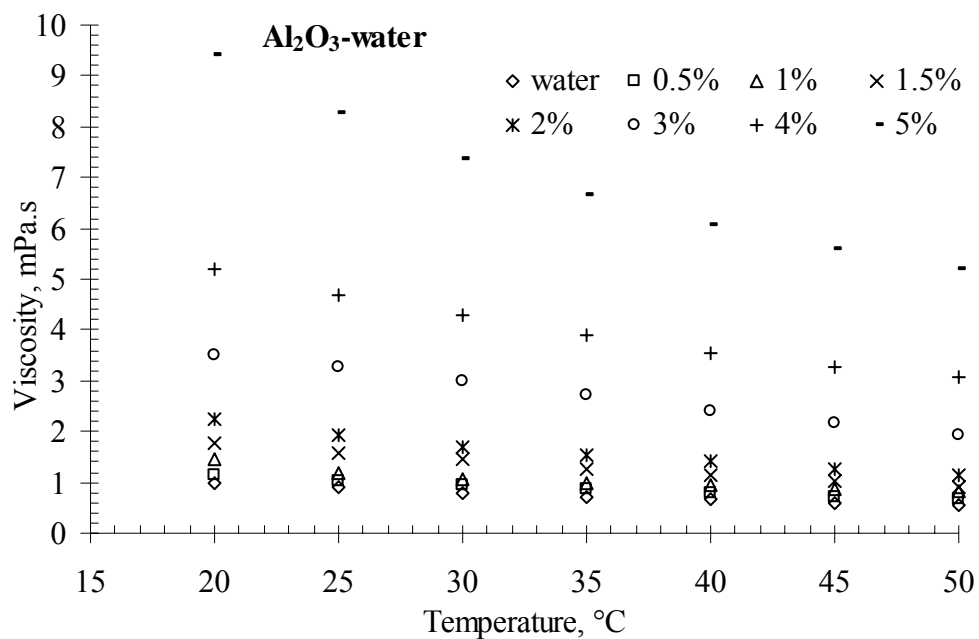


Figure 6.10 Effective viscosities of Al₂O₃-water nanofluids from 0.5 vol% to 5 vol% as a function of temperature

Comparison of the experimental results with Einstein, Krieger & Dougherty and Nielsen models is demonstrated in Figure 6.11. It may be seen that measured viscosity values are well above the prediction of the models, the difference becoming larger as the volume concentration is increasing.

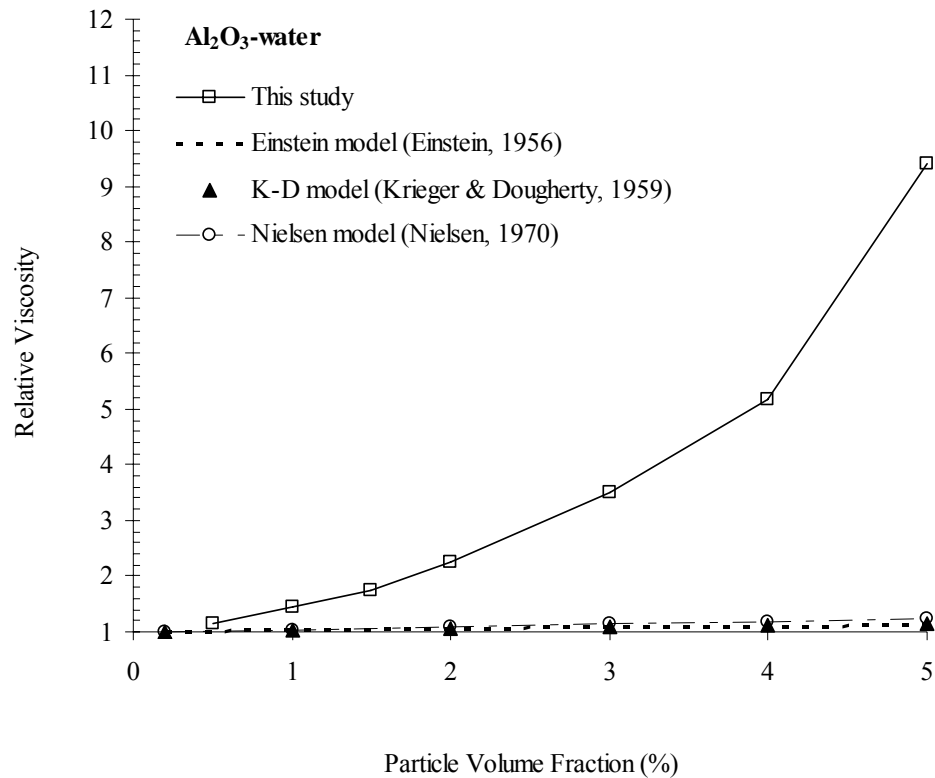


Figure. 6.11 Relative viscosity of Al₂O₃-water nanofluids as a function of nanoparticle volume fraction at 13 °C

In Figure 6.12 our experimental relative viscosity results are compared with the existing literature values for the same nanofluids by Pak & Cho (1998) for 13 nm, Wang et al. (1999) for 28 nm, Nguyen et al. (2007) for 47 nm and Lee et al. (2008) for 30 nm particle sizes. From figure it is seen that at 1 % particle volume fraction all the data are in the range of 1 – 1.5. Due to the increase in volume fraction two different tendencies are observed. On one hand our results and the values obtained by Pak & Cho (1998) indicate an increase in relative viscosity more than 8 fold, on the other hand this increment is less than 1 fold for the results of Nguyen et al. (2007) and Lee et al. (2008). Our results show very similar increments with the results of Pak & Cho (1998).

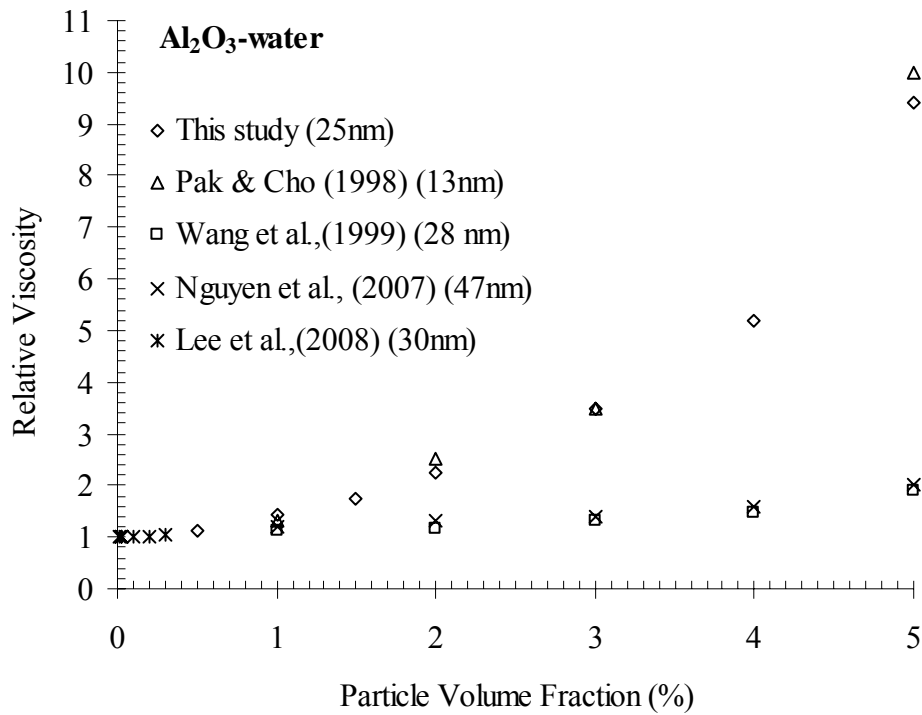


Figure 6.12 Experimental results of relative viscosity of Al₂O₃-water nanofluids for room temperature compared to selected literature data

6.4.1.4 Al₂O₃ – EG (Ethylene Glycol) Nanofluids

The effective viscosity of Al₂O₃-EG nanofluids with concentrations of 0.5 to 5.0 volume % were measured at temperatures from 20 °C to 50 °C and results are given in Table 6.3.

Table 6.4 Our experimental results for effective viscosity of Al₂O₃ – EG nanofluids (mPa.s)

Samples	Temperature (°C)				
	20	25	35	42	50
Ethylene glycol	20.9	16.1	10.7	9.00	6.55
Al ₂ O ₃ (0.5%)	21.5	17.5	11.4	9.09	6.63
Al ₂ O ₃ (1.0%)	23.5	20.2	13.2	10.7	7.60
Al ₂ O ₃ (2.0%)	28.4	23.3	15.6	12.9	9.00
Al ₂ O ₃ (3.0%)	35.6	29.9	20.2	16	11.5
Al ₂ O ₃ (4.0%)	48.4	40.5	27.6	20	15.2
Al ₂ O ₃ (5.0%)	67.4	47.7	31.2	24.5	17.8

Our experimental viscosity values for Al_2O_3 -EG nanofluids are also shown in Figure 6.13 according to temperature and particle volume fraction. Results show similar behavior as the results of water-based nanofluids. On one hand the viscosity of nanofluids increases dramatically, with an increase in particle concentration, on the other hand viscosity of these nanofluids show a similar decreasing behavior as ethylene glycol with the increase in temperature.

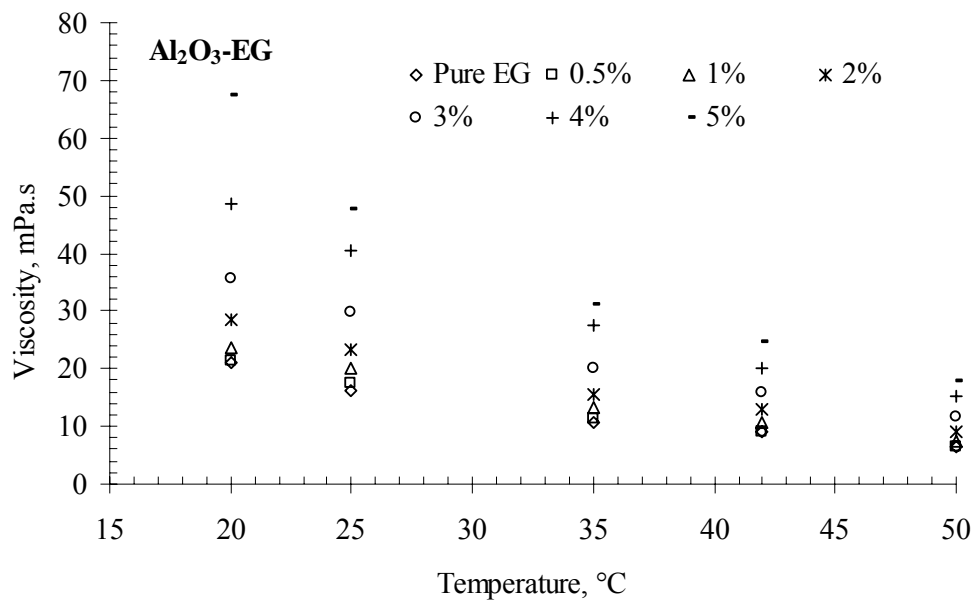


Figure 6.13 Effective viscosities of Al_2O_3 -EG nanofluids from 0.5 vol% to 5 vol% as a function of temperature

We compare our experimental results on Al_2O_3 -EG nanofluids with the models in Figure 6.14. Similar with the results of our water-based nanofluids, model predictions are very low compared with experimental data.

Our experimental relative viscosity results are compared with the existing literature values for the same nanofluids by Wang et al. (1999) for 28 nm, Timofeeva et al. (2007) for 20 nm and Anoop et al. (2009) for 100 nm particle sizes. From Figure 6.15 it is seen that at 1 % particle volume fraction all the data are in the range of 1 – 1.2. With the increase in volume fraction our results indicates a higher

enhancement with the data of Timofeeva et al. (2007), than the results of Wang et al. (1999) and Anoop et al. (2009).

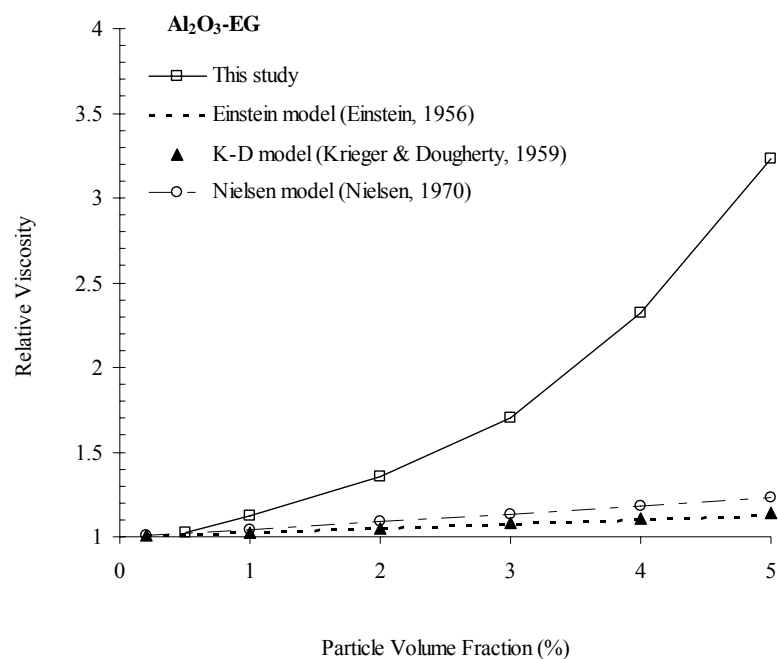


Fig. 6.14 Relative viscosity of Al₂O₃-EG nanofluids as a function of nanoparticle volume fraction at 20 °C.

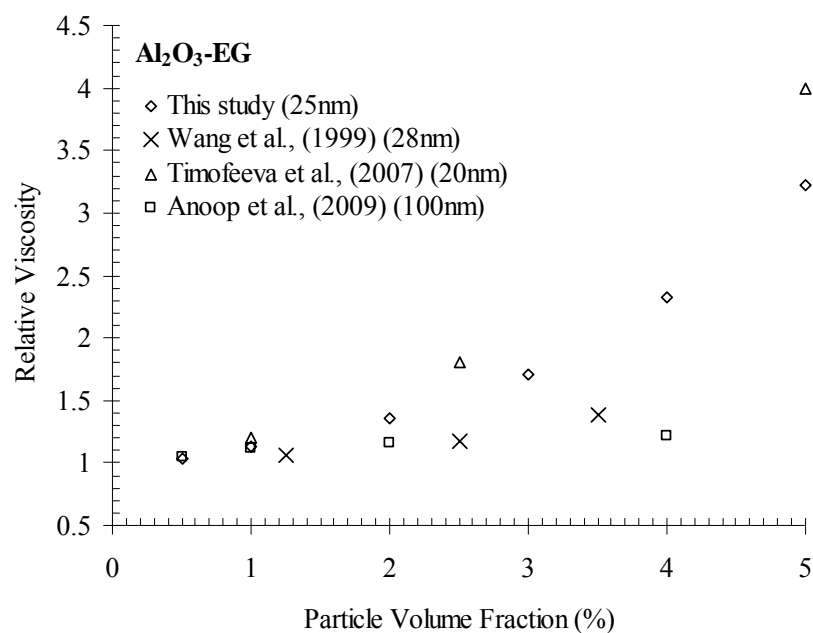


Figure 6.15 Experimental results of relative viscosity of Al₂O₃-EG nanofluids compared to selected literature data

6.4.2 Effect of Basefluid

For observing the effect of base-fluid on relative viscosity of nanofluids we compare our experimental results for Al_2O_3 -water and Al_2O_3 -EG nanofluids in Figure 6.16. As it is shown in the Figure relative viscosity of water based nanofluid is higher than the ethylene glycol based nanofluid. For 5 % particle volume fraction, relative viscosity of Al_2O_3 -water sample is almost two times higher than the Al_2O_3 -EG sample.

This result shows similarity with the effect of base-fluid on relative thermal conductivity of nanofluids that we concluded as for poorer (lower thermal conductivity) heat transfer fluid (ethylene glycol) the relative thermal conductivity was higher. For the base-fluid with the lower viscosity (water) increase in viscosity is much more than the base-fluid with higher viscosity (ethylene glycol).

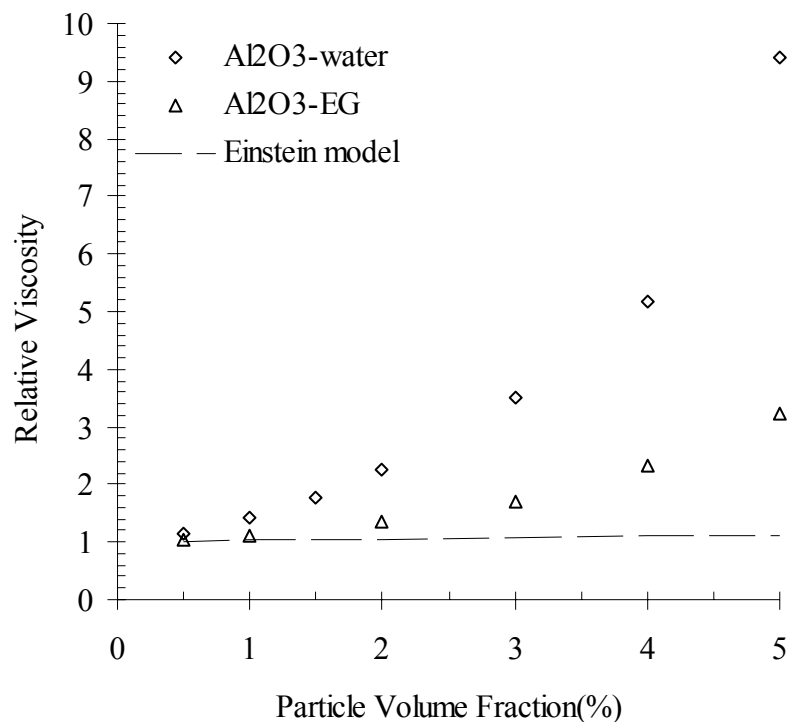


Figure 6.16 Experimental results of relative viscosity of Al_2O_3 -EG nanofluid compared to Al_2O_3 -water nanofluid.

6.5 Conclusion

Effective viscosities of SiO₂-water, TiO₂-water, Al₂O₃-water and Al₂O₃-EG nanofluids were measured using Sine-wave Vibro Viscometer at different particle concentrations and temperatures.

An 8 times increase in viscosity has been observed for 5% volume fraction of Al₂O₃-water nanofluid. This increase was the highest among the water-based nanofluids we have studied. For TiO₂-water nanofluids, the maximum increase was 135% for 3% of TiO₂ nanoparticle concentration by volume. For Al₂O₃-water nanofluids, the increase was 250% for the same nanoparticle concentration. For 4% volume fraction SiO₂-water nanofluid, the increase was 360%, whereas this increase was 418 % for Al₂O₃-water nanofluid for the same volume concentration.

These results show that viscosity of our nanofluids increase dramatically with the increase in particle concentration and classical effective viscosity models such as Einstein, Krieger & Dougherty and Nielsen are found to be unable to predict this increase. Also viscosity of these nanofluids, show a similar decreasing behavior as water or ethylene glycol with the increase in temperature.

Moreover the effect of base-fluid on relative thermal conductivity of nanofluids was investigated with two base-fluids, water and ethylene glycol. Al₂O₃ nanoparticles for volume fractions in the range of 0.5 % to 5.0 % were compared at 20°C. The results indicate that the enhancements ratio of the viscosity of ethylene glycol (EG) based nanofluids are smaller than those of water based nanofluids, showing a significant influence of the base fluid on the viscosity of the nanofluids.

This increase in effective viscosity with increasing particle concentration beyond the values predicted by classical models may be due to the possible agglomeration of the nanoparticles. Thus, big pumping powers are required to circulate the nanofluid in heat exchanger system. One must calculate the advantages gained by increased thermal conductivity of the use of nanofluid and see if this advantage is more

pronounced than the disadvantage of increased viscosity meaning bigger pumping power.

CHAPTER SEVEN

CONCLUSIONS

7.1 3- ω Method

We have built a hot wire sensor and developed a data reduction method for measurement of thermal conductivity of small quantities of liquid samples. The quantity of liquid required for thermal conductivity measurements is over 25 μl . The requirements for the validity of the theoretical analysis are easily fulfilled in practice. For frequencies below 1 Hz, the agreement between theory and experiment is good and justifies the assumptions of the theoretical section, including the condition $F \ll 1$.

As the frequency increases above 1 Hz, the deviation from the theoretical curves is apparent and is more pronounced in the signal phase. Except for the minimum sample volume there are no constraints on sample geometry. The thermal probe plays the role of excitation source and temperature sensor at the same time.

This probe is compact, reusable, low cost, and it is compatible with temperature dependent measurements. Due to ac modulation and lock-in signal processing, the long-term reproducibility of absolute value is 0.3% in k , in the case of relative measurements, the resolution is 0.1% in k . These values make the device very attractive for accurate thermophysical investigations of (nano)fluids.

Future work should focus on extending the feasible frequency range for 3 ω measurements by considering various more elaborate models for the heat transfer between the wire and the fluid. Moreover the application of the same ac hot wire method to soft solid composite materials should be tried both theoretically and experimentally.

7.2 Nanofluids

For homogenization, ultrasonic equipment was used after mixing of the nanoparticles to the base liquid. For the 50 ml nanofluid sample, all the samples were subjected to 110-120 Watts (2.2 – 2.4 W/mL) for 30 minutes. The key factor for the industrial application of nanofluids is their stability and uniform dispersion of nanoparticles in the basefluid. Zeta potential is an important parameter that reflects the colloid behavior of the particles. The measured zeta potential values of SiO₂ – water, TiO₂ – water, Al₂O₃ – water and Al₂O₃ – EG nanofluids were 30mV, 38 mV, 55 mV and 69 mV, respectively, which show that all our samples are physically stable.

The thermal conductivities of SiO₂-water, TiO₂-water, Al₂O₃-water and Al₂O₃-EG nanofluids were measured using a 3ω method for different particle concentrations and temperatures. The experimental results showed that the thermal conductivity enhancements were relatively in good agreement with the Hamilton-Crosser model. They were moderated increases, not as claimed by some researchers as anomalous increases.

From our results, we also noticed that, although thermal conductivity of Al₂O₃ was much higher than TiO₂, the thermal conductivities of TiO₂-water nanofluids were significantly higher than Al₂O₃-water nanofluids, which means that the thermal conductivity of the nanoparticles was not the only factor that determines the thermal conductivity of the nanofluids.

We also found that the relative thermal conductivity of the nanofluids was not dependent on temperature.

Although, it is suggested to use a surfactant by some researchers for preventing clustering of nanoparticles, we observed that the effect of sodium dodecylbenzenesulfonate (SDBS) surfactant was to decrease the thermal

conductivity of the base fluid. Thermal conductivity of Al_2O_3 – water nanofluids was better than with the same nanofluid with surfactant.

The effect of base-fluid on relative thermal conductivity of nanofluids was investigated with two base-fluids, water and ethylene glycol. Al_2O_3 nanoparticles for volume fractions in the range of 0.5 % to 5.0 % were compared. The results show that higher relative thermal conductivity for poorer (lower thermal conductivity) heat transfer fluid, ethylene glycol in this case.

The results of our experiments showed that the viscosity of nanofluids increase dramatically with the increase in particle concentration. To illustrate this, the increase in viscosity was 8 times greater than that of pure water for Al_2O_3 -water nanofluid with 5% volume fraction of particle. The classical effective viscosity models such as Einstein, Krieger & Dougherty and Nielsen are inadequate in explaining this great increase in viscosity.

For the nanofluids we have studied, viscosity decreased with increasing temperature in the same way as corresponding base fluids, water and ethylene glycol.

The effect of base-fluid on relative viscosity of nanofluids was investigated with two base-fluids, water and ethylene glycol. The results showed that the increase in relative viscosity was lower for ethylene glycol based nanofluids compared with water based nanofluids.

Finally, because of the large increase in effective viscosity, large pumping powers are required to circulate the nanofluid used in cooling systems. In order to have a good idea on the applicability of these nanofluids in real engineering systems, effective viscosity must be measured together with the thermal conductivity.

In fact the review of experimental studies clearly showed a lack of consistency in the reported results of various research groups. The effects of several important factors such as particle size and shapes, clustering of particles, temperature of the

fluid, and dissociation of surfactant on the effective thermal conductivity of nanofluids were not investigated adequately. It is very important that more investigations should be performed, in order to confirm the effects of these factors on the thermal conductivity for wide range of nanofluids.

However some standards for experimental research on nanofluids comprising preparation of nanofluids, stability of nanofluids, thermal conductivity and viscosity measurements of nanofluids should be brought. Moreover some blind identical samples could be sent to several groups for measurement of thermal conductivity and viscosity by similar and disparate methods.

REFERENCES

- Anoop, K. B., Kabelac, S., Sundararajan, T., & Das, S. K. (2009). Rheological and flow characteristics of nanofluids: Influence of electroviscous effects and particle agglomeration. *J. Appl. Phys.*, 106, 034909.
- Agop, M., Stan, C., Toma, M., & Rusu, I. (2007). Fractal space-time theory and some applications in advanced materials. In *Proceedings of the Romanian Academy Series A-Mathematics Physics Technical Sciences Information Science*, 8, 121-129.
- Assael, M. J., Chen, C. F., Metaxa, I., & Wakeham, W. A. (2004). Thermal conductivity of suspensions of carbon nanotubes in water. *Int. J. Thermophys.* 25, 971-985.
- Beck, M. P., Yuan, Y. H., Warriar, P., & Teja, A. S. (2009). The effect of particle size on the thermal conductivity of alumina nanofluids. *Journal of Nanoparticle Research*, 11, 1129-1136.
- Bhattacharya, P., Saha, S. K., Yadav, A., Phelan, P. E., & Prasher, R. S. (2004). Brownian dynamics simulation to determine the effective thermal conductivity of nanofluids. *J. of Applied Physics*, 95, 6492–6494.
- Bhattacharya, P., Nara, S., Vijayan, P., Tang, T., Lai, W., Phelan, P. E., Prasher, R. S., Song, D. W., & Wang, J. (2006). Characterization of the temperature oscillation technique to measure the thermal conductivity of fluids. *International Journal of Heat and Mass Transfer*, 49, 2950 – 2956.
- Biercuk, M. J., Llaguno, M. C., Radosavljevic, M., Hyun, J. K., Johnson, A. T., & Fischer, J. E. (2002). Carbon nanotube composites for thermal management. *Applied Physics Letters*, 80, 2767–2772.
- Birge, N. O., & Nagel, S. R. (1987). Wide-frequency specific heat spectrometer. *Rev. Sci. Instrum.*, 58, 1464 – 1470.

- Bruggeman, D. A. G. (1935). The calculation of various physical constants of heterogeneous substances I. The dielectric constants and conductivities of mixtures composed of isotropic substances. *Ann. Phys. (Leipzig)* 24, 636-664.
- Buzin, A. I., Kamasa, P., Pyda, M., & Wunderlich, B. (2002). Application of wollaston wire probe for quantitative thermal analysis. *Thermochim. Acta*, 381, 9-18.
- Cahill, D. G. (1990). Thermal conductivity measurement from 30 to 750 K: the 3 omega method. *Rev. Sci. Instrum.*, 61, 802 – 808.
- Carslaw, H. W., & Jaeger, J. C. (1959). *Conduction of Heat in Solids*, London: Oxford Univ. Press.
- Chandrasekar, M., & Suresh, S. (2009). A review on the mechanisms of heat transport in nanofluids. *Heat Transfer Engineering*, 30, 1136-1150.
- Chirtoc, M., Filip, X., Henry, J. F., Antoniow, J. S., Chirtoc, I., Dietzel, D., Meckenstock, R., & Pelzl, J. (2004). Thermal probe self-calibration in ac scanning thermal microscopy. *Superlattices and Microstructures*, 35, 305-314.
- Chirtoc, M., & Henry, J. F. (2008). 3ω hot wire method for micro-heat transfer measurements: From anemometry to scanning thermal microscopy (SThM). *Europ. Phys. J., Special Topics*, 153, 343-348.
- Choi, S. U. S. (1995). Enhancing thermal conductivity of fluids with nanoparticles. In *Developments and Applications of Non-Newtonian Flows*. (FED 231), (99–105). New York: American Society of Mechanical Engineers.
- Choi, S. U. S., Zhang, Z. G., Yu, W., Lockwood, F. E., & Grulke, E. A. (2001). Anomalous thermal conductivity enhancement in nano-tube suspensions. *Applied Physics Letters*, 79, 2252–2254.
- Choi, S. U. S. (2009). Nanofluids: From vision to reality through research, *J. Heat Transfer*, 131, 033106.

- Chon, C. H., Kihm, K. D. (2005). Thermal conductivity enhancement of nanofluids by Brownian motion. *J. Heat Transfer*, 127, 810.
- Dames, C., & Chen, G. (2005). 1ω , 2ω and 3ω methods for measurements of thermal properties, *Rev. Sci. Instrum.*, 76, 124902.
- Das, S. K., Putra, N., Thiesen, P., & Roetzel, W. (2003). Temperature dependence of thermal conductivity enhancement for nanofluids. *Journal of Heat Transfer*, 125, 567 – 574.
- Das, S. K., Putra, N., & Roetzel, W. (2003). Pool boiling characteristics of nanofluids. *Int. J. Heat Mass Transfer*, 46, 851–862.
- Das, S. K., Choi, S. U. S., Patel, H. E. (2006). Heat transfer in nanofluids—a review. *Heat Transfer Eng.*, 27, 2–19.
- Eastman, J. A., Choi, S. U. S., Li, S., & Thompson, L. J. (1997). Enhanced Thermal Conductivity through the Development of Nanofluids. In *Proc. Symp. on Nanophase and Nanocomposite Materials II*, Materials Research Society, Boston, 457, 3–11.
- Eastman J. A., Choi, S. U. S., Li, S., Yu, W., & Thompson, L. J. (2001). Anomalously increased effective thermal conductivities of ethylene glycol based nanofluids containing copper nanoparticles. *Applied Physics Letters*, 78, 718–720.
- Eastman, J. A., Phillpot, S. R., Choi S. U. S., & Keblinski, P. (2004). Thermal transport in nanofluids. *Annual Review of Materials Research*, 34, 219–246.
- Einstein, A. (1956). *Investigations on the Theory of the Brownian Movement*, Dover Publications, Inc., New York.
- Evans, W., Fish, J., & Keblinski, P. (2006). Role of Brownian motion hydrodynamics on nanofluid thermal conductivity. *App. Physics Lett.*, 88, 093116.

- Evans, W., Prasher, R., Fish, J., Meakin, P., Phelan, P., Keblinski, P. (2008). Effect of aggregation and interfacial thermal resistance on thermal conductivity of nanocomposites and colloidal nanofluids. *Int. J. of Heat and Mass Transfer*, 51, 1431-1438.
- Glory, J., Bonetti, M., Helezen, M., L'Hermite M. M., & Reynaud, C. (2008). Thermal and electrical conductivities of water-based nanofluids prepared with long multiwalled carbon nanotubes. *Journal of Applied Physics*, 103, 094309.
- Hamilton R. L., & Crosser O. K. (1962). Thermal conductivity of heterogeneous two component systems. *Industrial and Engineering Chemistry Fundamentals*, 1, 187–191.
- He, Y., Jin Y., Chen, H., Ding, Y., Cang, D., & Lu, H. (2007). Heat transfer and flow behaviour of aqueous suspensions of TiO₂ nanoparticles (nanofluids) flowing upward through a vertical pipe. *Int. J. Heat Mass Transfer*, 50, 2272 – 2281.
- Hong, K. S., Hong, T. K., & Yang H. S. (2006). Thermal conductivity of Fe nanofluids depending on cluster size of nanoparticles. *Applied Physics Letters*, 88, 031901.
- Hwang, Y. J. Ahn, Y. C., Shin, H. S., Lee, C. G., Kim, G. T., Park H. S., & Lee, J. K. (2006). Investigation on characteristics of thermal conductivity enhancement of nanofluids. *Current Applied Physics*, 6, 1068-1071.
- Izumo, N., & Koiwai, A. (2009). Technological background and latest market requirements concerning “static viscosity” measurement with a tuning-fork vibration viscometer. In Proceedings of Asia-Pacific Symposium on Measurement of Mass, Force and Torque (APMF 2009), 1-4 June 2009, Tokyo, Japan, 51-57.
- Jang, S. P., & Choi, S. U. S. (2004). Role of Brownian motion in the enhanced thermal conductivity of nanofluids. *App. Physics Lett.*, 84, 4316–4318.
- Kakac, S., & Pramuanjaroenkij, A. (2009). Review of convective heat transfer enhancement with nanofluids. *Int. J. Heat Mass Transfer*, 52, 3187 – 3196.

- Kang H. U., Kim S. H., & Oh J. M. (2006). Estimation of thermal conductivity of nanofluid using experimental effective particle volume. *Experimental Heat Transfer*, 19, 181-191.
- Kebllinski, P., Phillpot, S. R., Choi, S. U. S., & Eastman, J. A. (2002). Mechanisms of heat flow in suspensions of nano-sized particles (nanofluids). *Int. J. of Heat and Mass Transfer*, 45, 855–863.
- Kebllinski, P., Eastman J. A., & Cahill, D. G. (2005). Nanofluids for thermal transport. *Materials Today*, 8, 36–44.
- Kebllinski, P., Prasher, R., & Eapen, J. (2008). Thermal conductance of nanofluids: is the controversy over?. *J. Nanopart Res.*, 10, 1089–1097.
- Kostic, M. M. (2006). Critical issues and application potentials in nanofluids research. In *Proceedings of Multifunctional Nanocomposites*, 17036. Honolulu, Hawaii.
- Krieger, I. M., & Dougherty, T. J. (1959). A mechanism for non-Newtonian flow in suspensions of rigid spheres, *Journal of Rheology*, 3 (1), 137-152.
- Kwak K., & Kim, K. (2005). Viscosity and thermal conductivity of copper oxide nanofluid dispersed in ethylene glycol. *Korea–Australia Rheol. J.*, 17, 35-40.
- Lee, S., Choi, S. U. S., Li, S., & Eastman J. A. (1999). Measuring thermal conductivity of fluids containing oxide nanoparticles. *Journal of Heat Transfer*, 121, 280–289.
- Lee, J. H., Hwang, K. S., Jang, S. P., Lee, B. H., Kim, J. H., Choi, S. U. S., & Choi, C. J. (2008). Effective viscosities and thermal conductivities of aqueous nanofluids containing low volume concentrations of Al₂O₃ nanoparticles. *Int. J. Heat Mass Transfer*, 51, 2651-2656.

- Li, C. H., & Peterson, G. P. (2006). Experimental investigation of temperature and volume fraction variations on the effective thermal conductivity of nanoparticle suspensions (nanofluids). *Journal of Applied Physics*, 99, 084314.
- Li, C. H., Williams, W., Buongiorno, J., Hu, L. W., & Peterson G. P. (2008). Transient and steady-state experimental comparison study of effective thermal conductivity of Al₂O₃/water nanofluids. *J. Heat Transfer*, 130, 042407.
- Li, X. F., Zhu, D. S., Wang, X. J., Wang, N., Gao, J. V. and Li, H. (2008). Thermal conductivity enhancement dependent pH and chemical surfactant for Cu-H₂O nanofluids. *Thermochimica Acta*, 469, 98-103.
- Li, Y., Zhou, J., Tung, S., Schneider, E., & Xi, S. (2009). A review on development of nanofluid preparation and characterization. *Powder Technology*, 196, 89-101.
- Lide D. R. (2003). *Handbook of Chemistry and Physics*, 84th Edition, CRC Press, Boca Raton.
- Liu, M. S., Lin, M. C., Tsai, C. Y., & Wang, C. (2006). Enhancement of thermal conductivity with Cu for nanofluids using chemical reduction method. *Int. J. Heat Mass Transfer*, 49, 3028-3033.
- Masuda, H., Ebata, A., Teramae, K., & Hishinuma, N. (1993). Alteration of thermal conductivity and viscosity of liquid by dispersing ultra-fine particles (Dispersion of Al₂O₃, SiO₂, and TiO₂ ultra-fine particles). *Netsu Bussei (Japan)*, 7 (4), 227–233.
- Masoumi, N., Sohrabi, N., & Behzadmehr, A. (2009). A new model for calculating the effective viscosity of nanofluids. *Journal of Physics D-Applied Physics*, 42, 055501.
- Maxwell, J.C. (1881). *A Treatise on Electricity and Magnetism*. Oxford: Clarendon Press.

- Mintsas, H. A., Roy, G., Nguyen, C. T., & Doucet, D. (2009). New temperature dependent thermal conductivity data for water-based nanofluids. *Int. J. Therm. Sci.*, 48, 363-371.
- Murshed, S. M. S., Leong, K. C., & Yang, C. (2005). Enhanced thermal conductivity of TiO₂ - water based nanofluids. *International Journal of Thermal Science*, 44, 367-373.
- Murshed, S. M. S., Leong, K. C., Yang, C. (2008a), Thermophysical and electrokinetic properties of nanofluids-a critical review. *Appl. Therm. Eng.*, 28, 2109-2125.
- Murshed, S. M. S., Leong, K. C., & Yang, C. (2008b). Investigations of thermal conductivity and viscosity of nanofluids. *International Journal of Thermal Sciences*, 47, 560-568.
- Nagasaka, Y., & Nagashima, A. (1981). Absolute measurement of the thermal conductivity of electrically conducting liquids by the transient hot-wire method. *J. Phys. E: Sci. Instrum.*, 14, 1435 - 1440.
- Namburu, P. K., Kulkarni, D. P., Misra D., & Das, D. K. (2007). Viscosity of copper oxide nanoparticles dispersed in ethylene glycol and water mixture. *Exp Therm Fluid Sci*, 32, 397-402.
- Namburu, P. K., Kulkarni, D. P., Dandekar, A., & Das, D. K. (2007). Experimental investigation of viscosity and specific heat of silicon dioxide nanofluids. *Micro & Nano Letters*, 2(3), 67-71.
- Nielsen, L. E. (1970). Generalized equation for the elastic moduli of composite materials. *J. Appl. Phys.*, 41, 4626-4627.
- Nguyen, C. T., Desgranges, F., Roy, G., Galanis, N., Maré, T., Boucher, S., & Mintsas H.A. (2007). Temperature and particle-size dependent viscosity data for water-based nanofluids-hysteresis phenomenon. *Int. J. Heat Fluid Flow*, 28, 1492-1506.

- Ozerinc, S., Kakaç, S., Yazıcıoğlu, A. G. (2009). Enhanced thermal conductivity of nanofluids – A state-of-the-art review. *Microfluidics and Nanofluidics*, DOI: 10.1007/s10404-009-0524-4.
- Patel, H. E., Das, S. K., Sundararajan, T., Sreekumaran, N. A., George, B., Pradeep, T. (2003). Thermal conductivities of naked and monolayer protected metal nanoparticle based nanofluids: Manifestation of anomalous enhancement and chemical effects. *Applied Physics Letters*, 83, 2931–2933.
- Pak, B. C. & Cho, Y. I. (1998). Hydrodynamic and heat transfer study of dispersed fluids with submicron metallic oxide particles. *Exp. Heat Transfer*, 11, 151–170.
- Parker, W. J., Jenkins, R. J., Butler C. P., & Abbott, G. L. (1961). Flash method of determining thermal diffusivity, heat capacity, and thermal conductivity, *J Appl Phys.*, 32, 1679–1684.
- Powell, J. S. (1991). An instrument for the measurement of the thermal conductivity of liquids at high temperatures. *Meas. Sci. Technol.*, 2, 111 – 117.
- Prasher, R., Bhattacharya, P., & Phelan, P. E. (2005). Thermal conductivity of nanoscale colloidal solutions (nanofluids). *Physical Review Letters*, 94, 901/1–4.
- Prasher, R., Song, D., Wang, J., & Phelan, P. (2006). Measurements of nanofluid viscosity and its implications for thermal applications. *Appl. Phys. Lett.*, 89, 133108.
- Putnam, S. A, Cahill, D. G., Braun, P. V., & Shimmin, R. G. (2006). Thermal conductivity of nanoparticle suspensions. *Journal of Applied Physics*, 99, 084308.
- Putra, N., Roetzel, W., & Das, S. K. (2003). Natural convection of nanofluids. *Heat and Mass Transfer*, 39, 775–784.
- Ren, Y., Xie, H., & Cai, A. (2005). Effective thermal conductivity of nanofluids containing spherical nanoparticles. *J. Phys. D: Appl. Phys.*, 38, 3958–3961.

- Rusconi, R., Rodari, E., & Piazza, R. (2006). Optical measurements of the thermal properties of nanofluids. *Appl. Phys. Lett.*, 89, 261916.
- Sakonidou, E. P., van den Berg H. R. , ten Seldam C. A., & Sengers J. V. (1999). An improved guarded parallel-plate method for measuring the thermal conductivity of fluids in the critical region. *Int. J. Thermophys.*, 20, 1339-1366.
- Sarkar, S., & Selvam, R. P. (2007). Molecular dynamics simulation of effective thermal conductivity and study of enhanced thermal transport mechanism in nanofluids. *Journal of Applied Physics*, 102, 074302.
- Schmidt, A. J., Chiesa, M., Torchinsky, D. H., Johnson, J. A., Nelson, K. A., & Chen, G. (2008). Thermal conductivity of nanoparticle suspensions in insulating media measured with a transient optical grating and a hotwire. *J. Appl. Phys.*, 103, 083529.
- Shaikh, S., Lafdi, K., & Ponnappan, R. (2007). Thermal conductivity improvement in carbon nanoparticle doped PAO oil: An experimental study. *J. Appl. Phys.*, 101, 064302.
- Sinha, K., Kavlicoglu, B., Liu, Y., Gordaninejad, F., & Graeve O. A. (2009). A comparative study of thermal behavior of iron and copper nanofluids. *J. Appl. Phys.*, 106, 064307.
- Tillman, P., & Hill J. M. (2007). Determination of nanolayer thickness for a nanofluid. *Int. J. of Heat and Mass Transfer*, 34, 399-407.
- Timofeeva, E. V., Gavrilov, A. N., McCloskey, J. M., Tolmachev, Y. V., Sprunt, S., Lopatina, L. M., & Selinger, J. V. (2007). Thermal conductivity and particle agglomeration in alumina nanofluids: Experiment and theory. *Phys. Rev. E*, 76, 061203.
- Trisaksri, V. & Wongwises, S. (2007). Critical review of heat transfer characteristics of nanofluids. *Renewable and Sustainable Energy Reviews*, 11, 512-523.

- Vadasz, J. J., Govender, S., & Vadasz, P. (2005). Heat transfer enhancement in nanofluids suspensions: possible mechanisms and explanations. *Int. J. Heat Mass Transfer*, 48, 2673–2683.
- Venerus, D. C., Kabadi, M. S., Lee, S., & Perez-Luna, V. (2006). Study of thermal transport in nanoparticle suspensions using forced Rayleigh scattering. *J. Appl. Phys.*, 100, 094310.
- Wang, X., Xu, X., & Choi, S. U. S. (1999). Thermal conductivity of nanoparticle-fluid mixture. *Journal of Thermophysics and Heat Transfer*, 13, 474–480.
- Wang, B. X., Zhou, L. P., & Peng, X. F. (2003). A fractal model for predicting the effective thermal conductivity of liquid with suspension of nanoparticles. *Int. J. of Heat and Mass Transfer*, 46, 2665–2672.
- Wang, T., Luo, Z. Y., Shou, C. H., Zhang, S. B., & Cen K. F. (2007). Experimental study on convection heat transfer of nanocolloidal dispersion in a turbulent flow. *In Proceedings of the International Conference on Power Engineering 2007*, 993-998.
- Wang, X. Q. & Mujumdar, A. S. (2007). Heat transfer characteristic of nanofluids: a review. *Int. Journal of Thermal Sciences*, 46, 1-19.
- Wang, Z. L., Tang, D. W., Liu, S., Zheng, X. H., & Araki, N. (2007). Thermal-conductivity and thermal-diffusivity measurements of nanofluids by 3 ω method and mechanism analysis of heat transport. *Int. J. Thermophys.* 28, 1255-1268.
- Wen, D., & Ding, Y. (2004). Effective thermal conductivity of aqueous suspensions of carbon nanotubes (Carbon nanotube nanofluids). *J. Thermophys. Heat Transfer*, 18, 481–485.
- Wen, D., & Ding, Y. (2006). Natural convective heat transfer of suspensions of titanium Dioxide Nanoparticles (Nanofluids), *IEEE Transactions of Nanotechnology* 5(3), 220–227.

- Wen, D. S., Lin, G. P., Vafaei, S., & Zhang, K. (2009). Review of nanofluids for heat transfer applications. *Particuology*, 7, 141-150.
- Xie, H., Wang, J., Xi, T., Liu, Y., & Ai, F. (2002). Thermal conductivity enhancement of suspensions containing nanosized alumina particles. *Journal of Applied Physics*, 91, 4568-4572.
- Xie, H., Fujii, M., & Zhang, X. (2005). Effect of interfacial nanolayer on the effective thermal conductivity of nanoparticle-fluid mixture. *Int. J. of Heat and Mass Transfer*, 48, 2926-2932.
- Xuan, Y., & Li, Q. (2000). Heat transfer enhancement of nano-fluids. *International Journal of Heat and Fluid Flow*, 21, 58-64.
- Xuan, Y., Li, Q., & Hu, W. (2003). Aggregation structure and thermal conductivity of nanofluids. *AIChE J.*, 49, 1038-1043.
- Xue, Q. Z. (2003). Model for effective thermal conductivity of nanofluids, *Physics Letters A*, 307, 313-317.
- Xue, L., Keblinski, P., Phillpot, S. R., Choi, S. U. S., & Eastman, J. A. (2004). Effect of liquid layering at the liquid-solid interface on thermal transport. *Int. J. of Heat and Mass Transfer*, 47, 4277-4284.
- Yang, B., & Han, Z. H. (2006). Temperature-dependent thermal conductivity of nanorod-based nanofluids. *Appl. Phys.Lett.*, 89, 083111.
- Yoo D. H., Hong K. S., & Yang, H. S. (2007). Study of thermal conductivity of nanofluids for the application of heat transfer fluids. *Thermochimica Acta*, 455, 66-69.
- Yu, C. J., Richter, A. G., Datta, A., Durbin, M. K., & Dutta, P. (2000). Molecular layering in a liquid on a solid substrate: an X-ray reflectivity study. *Physica B*, 283, 27-31.

- Yu, W. and Choi, S. U. S. (2004). The role of interfacial layers in the enhanced thermal conductivity of nanofluids: A renovated Hamilton-Crosser model. *J. of Nanoparticle Research*, 6, 355–361.
- Yu, W. H., France, D. M., Routbort, J. L., & Choi, S. U. S., (2008). Review and comparison of nanofluid thermal conductivity and heat transfer enhancements. *Heat Transfer Engineering*, 29, 432 – 460.
- Zhang, X., Gu, H., & Fujii, M. (2006). Experimental study on the effective thermal conductivity and thermal diffusivity of nanofluids. *International Journal of Thermophysics*, 27, 569-580.
- Zhu, D. S., Li, X. F., Wang, N., Wang, X., Gao, J., & Li H. (2009). Dispersion behavior and thermal conductivity characteristics of Al₂O₃ –H₂O nanofluids. *Current Applied Physics*, 9, 131-139.